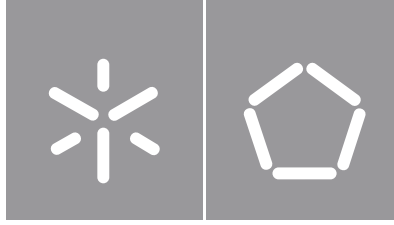




Universidade do Minho
Escola de Engenharia

Ana Carolina Lemos Gonçalves

**Biotechnological Applications of Odorant
Binding Proteins**



Universidade do Minho
Escola de Engenharia

Ana Carolina Lemos Gonçalves

Biotechnological Applications of Odorant Binding Proteins

Dissertação de Mestrado
Mestrado em Biotecnologia

Trabalho efetuado sob a orientação do
Doutor Artur Jorge Araújo Magalhães Ribeiro
e da
Doutora Carla Manuela Pereira Marinho da Silva

DIREITOS DE AUTOR E CONDIÇÕES DE UTILIZAÇÃO DO TRABALHO POR TERCEIROS

Este é um trabalho académico que pode ser utilizado por terceiros desde que respeitadas as regras e boas práticas internacionalmente aceites, no que concerne aos direitos de autor e direitos conexos.

Assim, o presente trabalho pode ser utilizado nos termos previstos na licença abaixo indicada.

Caso o utilizador necessite de permissão para poder fazer um uso do trabalho em condições não previstas no licenciamento indicado, deverá contactar o autor, através do RepositóriUM da Universidade do Minho.

Licença concedida aos utilizadores deste trabalho



Atribuição

CC BY

<https://creativecommons.org/licenses/by/4.0/>

AGRADECIMENTOS

A elaboração deste trabalho não teria sido possível sem a ajuda e incentivo de várias pessoas. Gostaria, portanto, de expressar toda a minha gratidão e apreço a todos aqueles que contribuíram para tornar esta tarefa mais fácil.

Em primeiro lugar, quero agradecer aos meus orientadores, Doutor Artur Ribeiro e Doutora Carla Silva, pelo apoio, motivação e todo o conhecimento partilhado. Obrigada por toda a ajuda e paciência nas horas menos boas, por todas as orientações prestadas que foram essenciais para a resolução desta dissertação.

Um agradecimento também para os membros do LBBN por toda a ajuda constante e por todos os concelhos. Um obrigado especial à Filipa, à Catarina ao David e ao André por estarem sempre disponíveis para esclarecer as dúvidas que surgissem e por toda a ajuda dada. Não poderia deixar de agradecer também às minhas colegas Mariana, Ana, Catarina, Mariana Castro e Sofia por me terem acompanhado durante este ano e por o terem tornado um pouco mais fácil e divertido.

Às minhas melhores amigas MJ e Beny, obrigada por todos estes anos de amizade, por nunca me deixarem desistir de nada e porque vocês tornam tudo mais bonito. À Sofia, porque os amigos não se medem em anos mas sim em momentos. À Marta e ao Diogo, por me obrigarem a treinar e me aturarem. Aos F.R.I.E.N.D.S., Simão, Gabi, Sérgio, Tomás e Marta, por estes dois anos difíceis graças ao mestrado mas incríveis. Às minhas afilhadas, Inês, Leonor e Marta por todo o apoio.

Gostava também de agradecer à minha psicóloga que foi muito essencial este ano.

Um obrigado enorme à minha mãe e a minha irmã porque não foi um ano fácil e mostraram-me o que é ser forte. À minha prima Filipa, que é um dos meus maiores exemplos, obrigada por todo o apoio e ensinamentos, és a irmã mais velha que nunca tive. Ao meu afilhado Lourenço, porque é das maiores alegrias da minha vida. Por fim, mas não menos importante, à minha avó e a minha amiga Cláudia que são os meus anjos da guarda. Espero que estejam orgulhosas de mim.

STATEMENT OF INTEGRITY

I hereby declare having conducted this academic work with integrity. I confirm that I have not used plagiarism or any form of undue use of information or falsification of results along the process leading to its elaboration.

I further declare that I have fully acknowledged the Code of Ethical Conduct of the University of Minho.

RESUMO

As proteínas de ligação a odores (OBPs) são pequenas proteínas da família das lipocalinas com a capacidade de se ligarem a moléculas odoríferas. As OBPs podem ser utilizadas em inúmeras áreas devido à boa estabilidade térmica, alta resistência a solventes orgânicos e à digestão proteolítica sua capacidade de ligar diferentes classes de odores, incluindo a detecção de substâncias perigosas.

Resultado da atividade diária e do exercício físico, o ser humano transpira e o que pode despoletar o desenvolvimento de odores desagradáveis. Neste trabalho, e com o intuito de diminuir o odor dos têxteis foram desenhadas 3 sequências de OBPs de porco, com capacidade de se ligar a tecidos de algodão e poliéster. Das 3 proteínas, designadas de OBP 1, OBP 2 e OBP 3 (por motivos de confidencialidade), apenas a OBP 1 e a OBP 2 expressaram, tendo a OBP 3 sido excluída do presente estudo. A caracterização físico-química das proteínas produzidas e da proteína wild-type (wt) foi realizada através das técnicas de MALDI-TOF, FTIR e Dicroísmo circular. Concluiu-se que a OBP1 e a OBP 2 apresentavam uma estrutura secundária diferente da OBP wild-type (wt) e que, quando aplicada uma temperatura superior a 60 °C, seguida de uma incubação a 4 °C, tanto a OBP 1 como a OBP 2 recuperavam a sua estrutura, fenómeno que não ocorreu com a OBP wt.

Foi estudada a ligação das proteínas a uma molécula modelo (1-AMA) e a fragrâncias (β -Citronellol, (-)-Menthol, Eugenol e Citronellil Valerate) e concluiu-se que a fragrância com melhor coeficiente de ligação ($<K_d$) às OBPs foi o β - Citronellol, pelo que foi a molécula selecionada para a funcionalização dos tecidos (algodão e poliéster).

Neste trabalho, foram propostas duas metodologias (impregnação e spray) para a funcionalização de têxteis com as OBPs (WT, OBP1 e OBP2), tendo-se obtido melhores resultados com o método de impregnação. Avaliou-se a libertação controlada de β - Citronellol das amostras funcionalizadas com OBPs, através da técnica de Cromatografia Gasosa (Headspace SPME/GC-MS). As amostras de tecido funcionalizadas pelo método de impregnação mostraram maior libertação de β - Citronellol.

Palavras-chave: proteínas de ligação a odores; libertação controlada de fragrâncias; redução de odores; têxteis inteligentes

ABSTRACT

Odor binding proteins (OBPs) are small proteins of the lipocalin family with the ability to bind odorant molecules. OBPs can be used in numerous areas due to their good thermal stability, high resistance to organic solvents and proteolytic digestion, their ability to bind different classes of odors, including the detection of hazardous substances.

Due to daily activity and physical exercise, the human being sweats and this can trigger the development of unpleasant odors. In this work, and to reduce the odor of textiles, 3 sequences of pig OBPs were designed, with the ability to bind to cotton and polyester fabrics. Of the 3 proteins, designated OBP 1, OBP 2 and OBP 3 (for confidentiality reasons), only OBP 1 and OBP 2 expressed, and OBP 3 was excluded from the present study. The physical-chemical characterization of the proteins produced and the wild-type protein (wt) was performed using the MALDI-TOF, FTIR and Circular Dichroism techniques. It was concluded that OBP1 and OBP 2 had a secondary structure different from wild-type (wt) OBP and that, when applied at a temperature above 60 °C, followed by an incubation at 4 °C, both OBP 1 and OBP the OBP 2 recovered their structure, a phenomenon that did not occur with the OBP wt.

The binding of proteins to a model molecule (1-AMA) and to fragrances (β -Citronellol, (-)-Menthol, Eugenol and Citronellil Valerate) was studied and it was concluded that the fragrance with the best binding coefficient ($<K_d$) β -Citronellol was added to the OBPs, so it was the molecule selected for the functionalization of fabrics (cotton and polyester).

In this work, two methodologies were proposed (impregnation and spray) for the functionalization of textiles with the OBPs (WT, OBP1 and OBP2), having obtained better results with the impregnation method. The controlled release of β -Citronellol from samples functionalized with OBPs was evaluated using the Gas Chromatography technique (Headspace SPME/GC-MS). The fabric samples functionalized by the impregnation method showed greater release of β -Citronellol.

Keywords: odor binding proteins; fragrance release; odor reduction; smart textiles.

LIST OF CONTENTS

AGRADECIMENTOS	iii
RESUMO	v
ABSTRACT	vi
LIST OF ABBREVIATIONS	ix
LIST OF FIGURES.....	x
LIST OF TABLES.....	xiii
1. STATE OF THE ART	1
1.1. Olfactory system	1
1.2. What are OBPs	1
1.3. Discovery and importance	4
1.4. Structure of OBPs	5
1.5. Binding Affinity of OBPs	6
1.6. Applications.....	7
1.6.1. Biosensors.....	8
1.6.2. Capture and release of odors	10
1.6.3. Textile industry.....	13
1.7. Challenges	14
2. AIMS	15
3. MATERIALS AND METHODS	16
3.1. Expression of OBPs.....	16
3.1.1. Transformation of <i>E. coli</i> BL21 (DE3) strain.....	16
3.1.2. Screening of protein expression.....	17
3.1.3. OBPs production and purification	18
3.2. Characterization of OBPs.....	19
3.2.1. MALDI-TOF	19
3.2.2. FITR	19
3.2.3. Circular Dichroism	20

3.3.	OBPs' Binding Performance	20
3.3.1.	Ligand Binding Assays	20
3.3.2.	Competitive Binding Assays.....	21
3.4.	Functionalization of textile substrates with OBP	22
3.4.1.	Functionalization of textiles.....	22
3.4.2.	Fragrance release from functionalized fabrics	24
4.	RESULTS AND DISCUSSION	26
4.1.	Transformation of <i>E. coli</i> BL21 (DE3).....	26
4.1.1.	Screening of protein expression	26
4.2.	OBP expression and purification	28
4.2.1.	Purification with nickel magnetic beads	29
4.2.2.	Dialysis and Freeze drying.....	29
4.3.	Characterization of OBPs.....	30
4.3.1.	MALDI-TOF	30
4.3.2.	FITR	30
4.3.3.	Circular Dichroism	31
4.4.	OBPs' Binding Performance	34
4.4.1.	Ligand Binding Assays	34
4.4.2.	Competitive Binding Assays.....	35
4.5.	Functionalization of textile substrates with OBPs	36
4.5.1.	Functionalization of fabrics.....	36
4.5.2.	Evaluation of fragrance release from functionalized fabrics.....	40
5.	CONCLUSION	44
6.	REFERENCES	46
7.	Supplementary Information.....	53
7.1.	Calibration curve of β -Citronellol:.....	53
7.2.	GC data	54

LIST OF ABBREVIATIONS

1-AMA	1-aminoanthracene
CD	Circular Dichroism
DMSO	Dimethyl sulfoxide
E. coli	<i>Escherichia coli</i>
FTIR	Fourier transform infrared spectroscopy
GC-MS	Gas chromatography–mass spectrometry
IC50	Inhibitory concentration
IPTG	Isopropyl β -D-1-thioXZXactopyranoside
K_a	Association constant
K_d	Dissociation constant
LB	Lysogeny broth
MALDI-TOF	Matrix-assisted laser desorption/ionization with time-of-flight
OBP	Odorant Binding Protein
OD	Optic Density
PI	Isoelectric Point
pOBP	Pig Odorand Binding Protein
SDS-PAGE	Sodium dodecyl sulfate-polyacrylamide gel electrophoresis
SPME	Solid Phase Microextraction
TB-AIM	Auto induction Terrific Broth
TSS	Transformation and Storage Solution

LIST OF FIGURES

<p>Figure 1- Cartoon diagram of the porcine OBP. The figure indicates the localization of Trp16 residue (red, W16), five Tyr residues (blue, Y20, Y52, Y78, Y82 and Y92), and the disulfide bridge between Cys63 and Cys155 (yellow). Figure taken from Staiano et al. (2007), 200756, constructed based on pOBP structure given in file 1A3Y.pdb.</p>	2
<p>Figure 2- Mechanism of mammalian olfactory system. (1) odorant-binding proteins (OBPs) present in the nasal mucus (2) olfactory receptors (ORs) present in olfactory neuronal cell). (3) G-protein (4) production of cyclic nucleotide (cAMP) by the activation of adenylyl cyclase (AC) (5) inflow of Ca²⁺ and Na⁺ ions which increase inside of neuronal cell causes an efflux of Cl⁻ (6) brain. Figure taken from Gonçalves et al. (2021).</p>	3
<p>Figure 3- Mechanism of insect's olfactory system. Figure taken from Brito et al. (2016). 3</p>	3
<p>Figure 4- Vertebrate OBPs. Figure taken from Gonçalves et al. (2021).</p>	4
<p>Figure 5- Three-dimensional structure and amino acid sequence of bovine and pig OBPs. Figure taken from Pelosi et al. (2014).....</p>	5
<p>Figure 6- (A) Experimental procedure to evaluate the amount of 1-AMA transduced into the liposomes and bound to protein-functionalized liposomes. After incubation of liposomes with 1-AMA at 37 °C, the free ligand is removed using a gel filtration chromatography column with a 5 kDa cutoff. The amount of 1-AMA in the liposomes was measured by the fluorescence emission at 600 nm. Figure taken from Gonçalves, Silva, et al. (2018) (B) Experimental layout for competitive binding evaluation. Figure taken from Gonçalves et al. (2018).....</p>	7
<p>Figure 7- Properties and applications of mammalian OBPs. Figure was based on Gonçalves et al. (2021).</p>	8
<p>Figure 8- Pig OBPs fused to three cell-penetrating peptides. Figure taken from Gonçalves et al. (2018).</p>	11
<p>Figure 9- Representation of an anchorage-based system composed by fusion OBPs and liposomes for the entrapment and transport of molecules. Figure taken from Gonçalves et al. (2018).</p>	11
<p>Figure 10- Opposite temperature-dependent affinities of tOBP and OBP:GQ20: SP-DS3 to 1-aminoanthracene (1-AMA). (a) Different binding affinities of tOBP and OBP:GQ20: SP- S3 (b) OBP's competitive temperature-dependent mechanism. Figure taken from (Gonçalves et al., 2018).....</p>	12

Figure 11- Release of fragrance from OBP-functionalized cotton, triggered by sweat. The release of fragrance was measured by GC-MS. The figure was taken from Goncalves et al. (2019).	13
Figure 12- Functionalization of textiles by impregnation method.	23
Figure 13- Functionalization of textiles by spray method.	24
Figure 14- SDS-PAGE (12%) electrophoresis of different proteins expressed in TB-AIM at 37 °C, 200 rpm. (A) OBP 1 (B) OBP 2 (C) OBP 3.....	26
Figure 15- SDS-PAGE (12%) electrophoresis of OBP 1, OBP 2 and 3, incubated in TB-AIM at different temperatures and 200 rpm. (A) 30 °C (B) 25 °C (C)18 °C.	27
Figure 16- SDS-PAGE (12%) electrophoresis of the soluble or insoluble fraction of OBP 1.	28
Figure 17- SDS-PAGE (12%) electrophoresis of: A) OBP 1 purified with nickel magnetic beads and eluted with increasing imidazole concentrations; B) OBP 2 purified with nickel magnetic beads and eluted with increasing imidazole concentrations.	29
Figure 18- (A) Protein yield after purification (B) proteins after lyophilization.	29
Figure 19- FTIR spectra of the OBP wt, OBP 1 and OBP 2 at amide I peak (1600- 1700cm ⁻¹).	30
Figure 20- Circular Dichroism spectra of OBP wt, OBP 1, and OBP2. The spectra were obtained by inserting the data of each protein providing from Jasco J-1500 spectropolarimeter in GraphPad.	33
Figure 21- K/S evaluation of fabrics functionalized with OBPs using method 1 (Impregnation). Control samples were done with the fabric without any functionalization.	37
Figure 22- K/S evaluation of polyester fabrics functionalized using method 1 (Impregnation) with OBPs before and after 1, 3, 5, 10 and 20 washes. Control samples were done with the fabric without any functionalization.	38
Figure 23- K/S evaluation of polyester fabrics functionalized with OBPs at different temperatures using method 2 (Spraying) and after different washes. Control samples were done with the fabric without any functionalization.	39
Figure 24- K/S evaluation of polyester fabrics functionalized with OBPs using method 1: impregnation at 70 °C and method 2: Spray at 120 °C and after different washes. Control samples were done with the fabric without any functionalization.	40

Figure 25- Evaluation of β -Citronellol release from OBPs after functionalization using method 1 (Impregnation) and method 2 (Spray), before washes and after washes.....	42
Figure 26- Evaluation of β -Citronellol lost between washes for samples functionalized using in method 1 (Impregnation) and method 2 (Spray).....	43
Figure SI 1- Calibration curve of β -Citronellol at 37 °C for 2 h of SPME exposition time.	53
Figure SI 2- GC spectra of polyester fabric incubated with β - citronellol at 37 °C for 2 h of SPME exposition time at 37 °C for 2 h of SPME exposition time	54
Figure SI 3- GC spectra of polyester fabric incubated at 37 °C for 2 h of SPME exposition time at 37 °C for 2 h of SPME exposition time.	54
Figure SI 4- GC spectra from functionalization of polyester fabrics with OBP/ β - citronellol complex by method 1; impregnation incubated at 37 °C for 2 h of SPME exposition time.....	56
Figure SI 5- GC spectra from functionalization of polyester fabrics with OBP/ β - citronellol complex by method 2: Spray incubated at 37 °C for 2 h of SPME exposition time.	57

LIST OF TABLES

Table 1- Theoretical molecular weight of each protein.....	17
Table 2- Composition of running and stacking gel in SDS-PAGE.....	18
Table 3- Number of colonies and transformation efficiency of OBPs	26
Table 4- Cell culture medium and temperatures tested for the expression of OBP Proteins	28
Table 5- Theoretical (by SnapGene® 3.0.3) and experimental (by MALDI-TOF) molecular weight of OBPs	30
Table 6- Resulting discrete peaks, their respective contribution to the overall FTIR-derived curves and the corresponding structural assignments of OBP proteins. Structural assignment was performed according to KONG and YU (2007)	31
Table 7- 1-AMA binding dissociation constants (Kd) of OBPs.	35
Table 8- OBP-Fragrance dissociation constants (Kd).....	36

1. STATE OF THE ART

1.1. Olfactory system

Smell is a common sense in the animal kingdom. It can be found in mammals, insects, fish, etc. It has a fundamental role in the identification of predators and prey, location of food sources or toxic foods, reproduction purposes, among others (Tegoni et al., 2000; Brito et al., 2016; Archunan, 2018). In 1991, Buck and Axel cloned and characterized 18 different members of an extremely large multigene family that encodes seven transmembrane domain proteins whose expression is restricted to the olfactory epithelium and discovered mammals' olfactory receptors cloning. These olfactory receptors belong to the class of 7-helix transmembrane G protein-coupled receptors and fall into several subfamilies and due to the diversity of these receptors, it is possible that mammals recognize many different odorant molecules (Buck and Axel, 1991).

The olfactory receptors are separated from the air by a protective layer of hydrophilic secretion, the nasal mucus in mammals, and the sensillar lymph in insects, therefore, odorant molecules cannot easily cross the hydrophilic barrier of the nasal mucus (Tegoni et al., 2000). Pelosi et al. (1982) discovered a soluble pyrazine-binding protein, which is secreted by the nasal olfactory mucosa of bovines and other mammals. The abundance of this protein in the nasal mucus of these animals has given rise to the hypothesis that it can serve as an odor carrier, and for this reason it has been called odorant binding protein (OBP). The smelling process is dependent on a synergistic mechanism that exists between the odorant, odorant binding proteins (OBPs) and the olfactory receptors (OR) (Alfinito et al., 2010; Barbosa et al., 2018).

1.2. What are OBPs

Odorant binding proteins are small molecular weight proteins (**figure 1**) members of the lipocalins superfamily with capacity of binding differentiated molecules and pass through the hydrophilic nasal mucus of vertebrates or the lymph of insect chemosensory sensilla until reaching the olfactory receptors (Wang et al., 2021). These proteins are present in large quantities on the tissues of the respiratory and olfactory mucosa can also be involved in general defense mechanisms in mammals, such as removing harmful substances from the air they breathe (Anderson, 1988; Boudjelal et al., 1996).

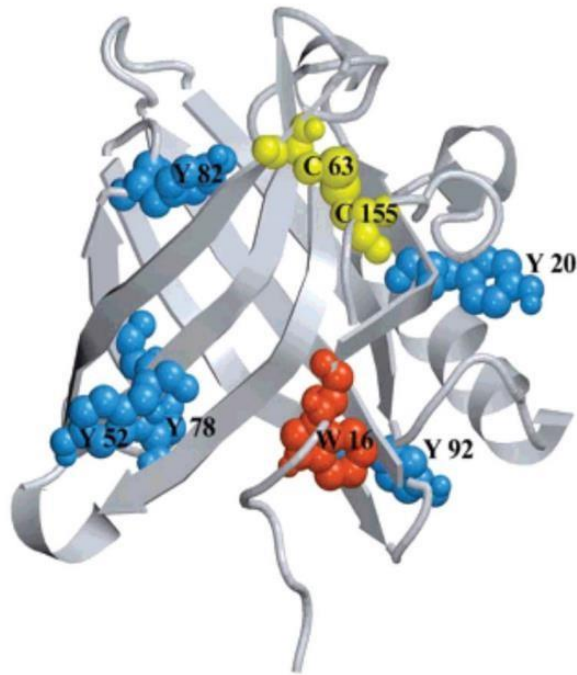


Figure 1- Cartoon diagram of the porcine OBP. The figure indicates the localization of Trp16 residue (red, W16), five Tyr residues (blue, Y20, Y52, Y78, Y82 and Y92), and the disulfide bridge between Cys63 and Cys155 (yellow). Figure taken from Staiano et al. (2007), 200756, constructed based on pOBP structure given in file 1A3Y.pdb.

They feature extremely stable architectures at different temperatures, organic solvents and proteolytic digestion, which make OBPs suitable elements for the manufacture of biosensors for food, agriculture and textile industries, medical applications and detection of dangerous substances, as well as for other biotechnological applications (Pelosi et al., 2014). Despite their function not being yet precise, these proteins are considered to be the carriers of odorants through the nasal mucosa of mammals and sensory lymph to ORs in the sensory neurons (Silva et al., 2014; Wang et al., 2021).

OBPs can be found in the nasal mucosa of mammals (**figure 2**). When in presence of odorant molecules, these proteins are responsible for their transport to the ORs, present in the olfactory sensory cells. This will originate a cascade of intracellular signaling that will be triggered by a G protein and consequently will lead to the production of cyclic nucleotide (cAMP), by the activation of adenylyl cyclase (AC). The flow of ions Ca^{2+} and Na^{+} will be induced by cAMP inside the neuronal cells and cause an efflux of Cl^{-} contributing to the depolarization of the olfactory neuron, leading to the modification of the action potential that is conducted along the axon until the olfactory bulb where the olfactory signal is interpreted by the brain (Gonçalves et al., 2021).

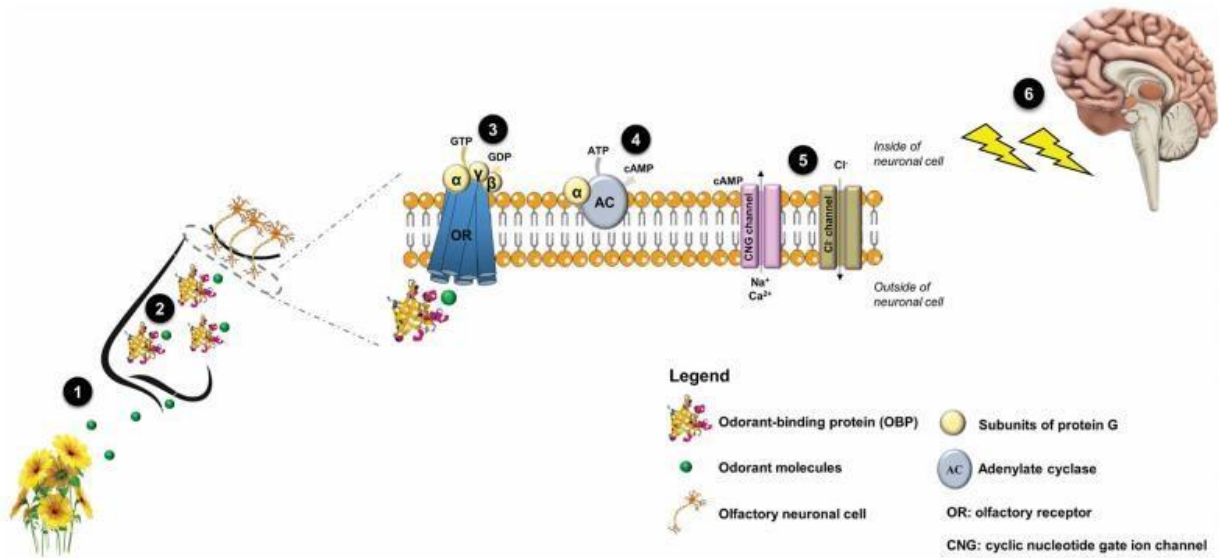


Figure 2- Mechanism of mammalian olfactory system. **(1)** odorant-binding proteins (OBPs) present in the nasal mucus **(2)** olfactory receptors (ORs) present in olfactory neuronal cell. **(3)** G- protein **(4)** production of cyclic nucleotide (cAMP) by the activation of adenylate cyclase (AC) **(5)** inflow of Ca²⁺ and Na⁺ ions which increase inside of neuronal cell causes an efflux of Cl⁻ **(6)** brain. Figure taken from Gonçalves et al. (2021).

In insects, OBPs are synthesized inside the olfactory sensilla by specialized accessory cells and secreted into the sensilla lymph, where they are found in high concentrations. Olfactory sensilla are delicate, hair-like porous cuticular structures located on the antennae. OBPs bind and solubilize odorants as they enter the porous tubules of the sensilla. Thereafter, they are transported through the sensillar lymph to the sensory dendrites, where they activate membrane bound ORs (**figure 3**) (Brito et al., 2016).

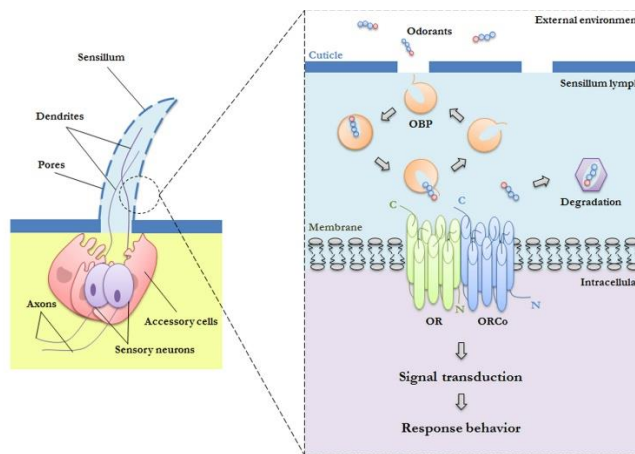


Figure 3- Mechanism of insect's olfactory system. Figure taken from Brito et al. (2016).

1.3. Discovery and importance

OBPs are small (around 15-20 kDa), hydrophilic proteins that are highly expressed in the glands of nasal mucosa of mammals and in the lymph of insect chemosensory sensilla (Brito et al., 2016; Gonçalves et al., 2021).

In 1985 the first vertebrate OBP was identified and isolated from the bovine nasal mucus (Bignetti et al., 1985). The bovine OBP to be purified was the pyrazine-binding protein that came from the nasal mucosa of mammals and was first discovered using ligand-binding assays with 2-isobutyl-3-methoxypyrazine, a very powerful green-smelling component of bell peppers. It was thought that this protein could only be an olfactory marker, however the pyrazine-binding protein is very different from the olfactory marker protein since no cross-reaction with antisera was observed (Bignetti et al., 1985).

Other vertebrate OBPs have been identified afterwards (**figure 4**) (Gonçalves et al., 2021). These proteins are expressed, during vertebrates' life, however only during certain periods and under specific physiological conditions, meaning that their rate of production is not constant (Pelosi, 2001).

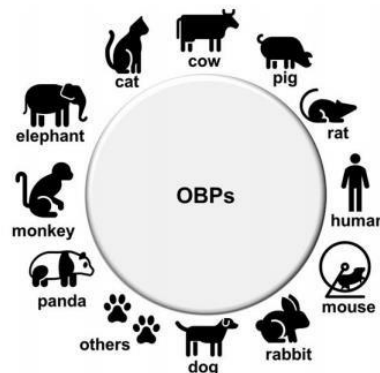


Figure 4- Vertebrate OBPs. Figure taken from Gonçalves et al. (2021).

Lacazette et al. (2000) reported for the first time the identification of human lipocalins involved in the binding of odorants. They investigated whether human lacrimal lipocalins would be produced from two active genes and found a new family of parallel genes on human chromosome 9q34, created by recent genomic duplications. The authors concluded that the biochemical characteristics of lipocalins have been applied to several physiological functions, mainly via new genes, but they can also be applied via recruitment of previous genes acquiring new functions in different organs.

The exact function of OBPs is not yet clear, but these proteins have been described in several processes related to the binding and presentation of odors. These proteins are believed to be responsible for transporting odorant molecules through the watery mucus barrier towards the olfactory receptors as they are secreted in the nasal mucosa (Gonçalves et al., 2021). OBPs can be easily expressed in bacterial systems and purified at low cost, being though useful in biotechnological applications.

1.4. Structure of OBPs

OBPs belong to the family of lipocalin proteins, that include carrier proteins, such as retinol-binding protein, β -lactoglobulin and other proteins. Mammalian and insect OBPs possess totally different three-dimensional structures even though they have similar functions (Gaubert et al., 2020). Insect OBPs assemble a core of six α -helices held together by three disulfide bridges, while mammalian OBPs have a three-dimensional structure with eight antiparallel β -sheets and a short α -helical segment close to the C terminal, similarly to the other lipocalins. Most OBPs contain 6 cysteines that form an asymmetric pattern, which is useful for their identification, however, these cysteine residues do not play an important role in the stability of vertebrate OBPs (Pelosi et al., 2014; Vogt & Carolina, 2005). In **figure 5** the three-dimensional structure of two mammalian OBPs, bovine and pig OBPs, is represented (Paolo Pelosi et al., 2014). Bovine OBP does not contain cysteines being a homodimer, while pig OBP presents two cysteine residues forming a dimeric structure (Guex & Peitsch, 1997).

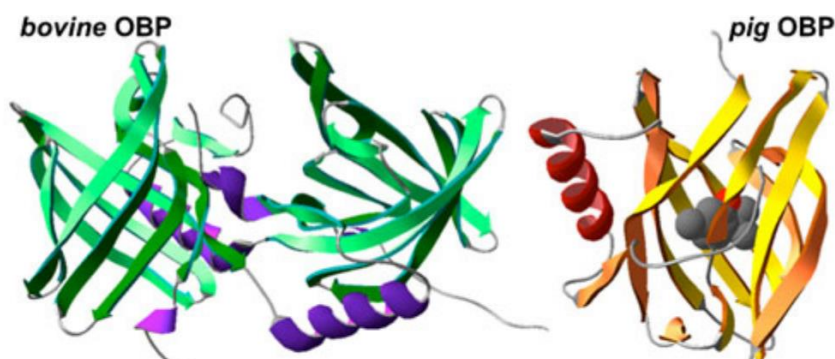


Figure 5- Three-dimensional structure and amino acid sequence of bovine and pig OBPs. Figure taken from Pelosi et al. (2014).

1.5. Binding Affinity of OBPs

The first OBP binding assays were performed using radiolabeled ligands and techniques like electrophoresis and gel filtrations to separate bound and free ligands (Pelosi et al., 2014, 2018). Over time, these radioactive ligand labels were improved and fluorescent probes were developed to measure the affinity of odorants to these proteins (Pelosi et al., 2018).

There are three methods to study the binding and to monitor the binding process of a ligand to OBP proteins. Two are based on the difference between the initial amount of ligand that was added to the reaction and the amount of free ligand after separation. In the first method, the free ligand is separated by several centrifugations and then quantified and in the second method, the OBP complex /free ligand is separated by dialysis. The third method does not require any separation step being a faster method where the results are less subject to measurement errors. This method consists on the addition of a fluorescent ligand that makes possible to determine the OBP/ligand complex directly (Pelosi et al., 2018).

1-Aminoanthracene is a fluorescent ligand widely used to evaluate the formation of OBP/ligand complexes (**figure 6 A**) (Gonçalves, Silva, et al., 2018). Paolini et al. (1999) used this ligand for the first time to measure the activity of pig OBP. The fluorescence was measured with an excitation wavelength of 295 nm whereas the maximum wavelength of 481 nm.

The affinity of non-fluorescent ligands to OBPs can be determined due to their ability to compete with a fluorescent ligand. In competitive binding experiments (**figure 6 B**), the protein is incubated with the fluorescent ligand at a fixed concentration and then increasing amounts of a non-fluorescent ligand are added (Gonçalves et al., 2018; Paolini et al., 1999). The higher the ability of the non-fluorescent ligand to bind the OBP and replace the fluorescence probe the higher its affinity to the protein. Despite not being effectively scientifically defined, some authors report that the best ligands have a dissociation constant (K_d) between 0.1 and 1.0 μM (Tegoni et al., 2000).

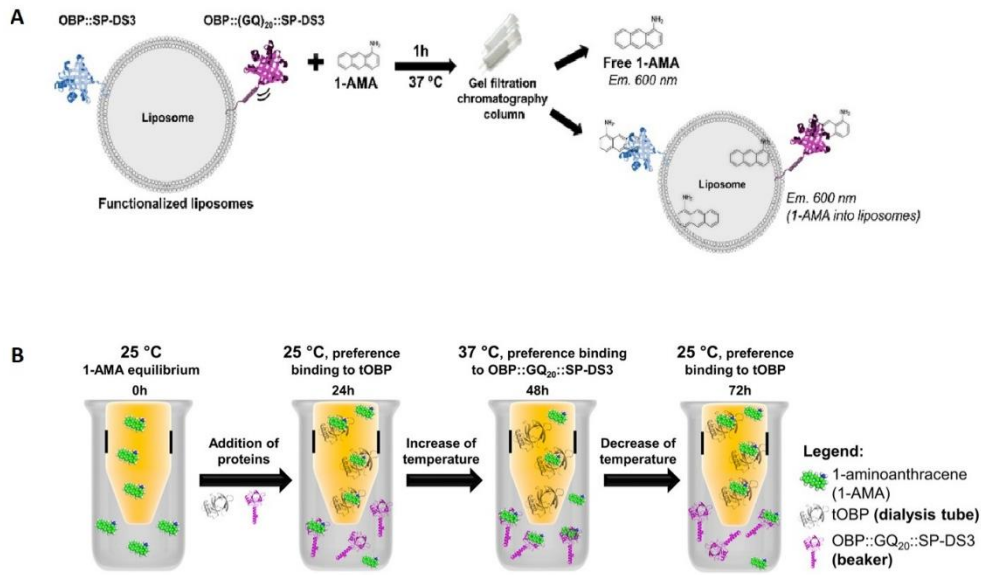


Figure 6- (A) Experimental procedure to evaluate the amount of 1-AMA transduced into the liposomes and bound to protein-functionalized liposomes. After incubation of liposomes with 1-AMA at 37 °C, the free ligand is removed using a gel filtration chromatography column with a 5 kDa cutoff. The amount of 1-AMA in the liposomes was measured by the fluorescence emission at 600 nm. Figure taken from Gonçalves, Silva, et al. (2018) **(B)** Experimental layout for competitive binding evaluation. Figure taken from Gonçalves et al. (2018).

1.6. Applications

Due to their specific properties, great stability and possibility to be tailored using molecular biology tools, OBPs have been applied in the most diverse fields of application, namely in biosensors development, food and water quality analysis, detection of hazard substances and in the capture and release of odorant molecules (**figure 7**).

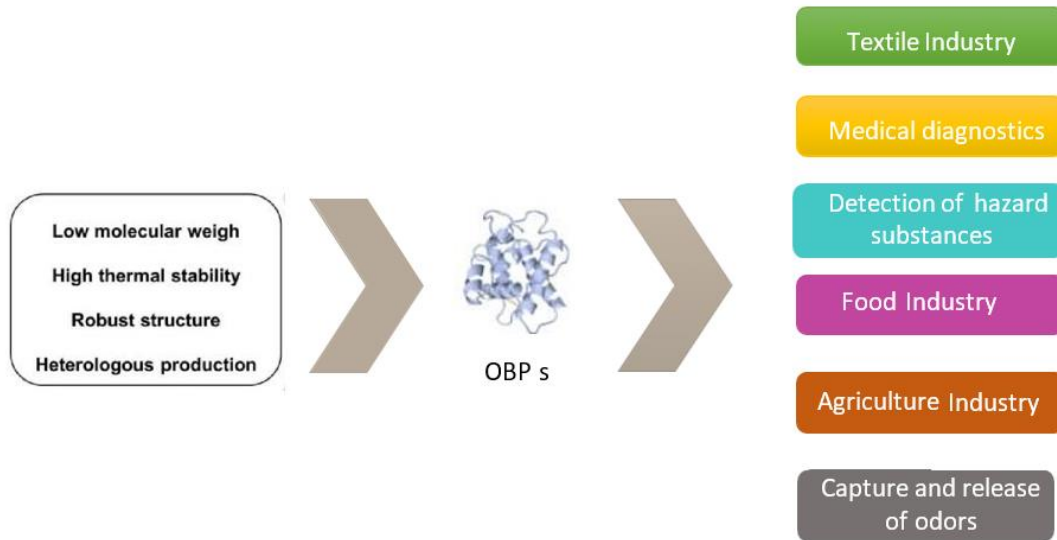


Figure 7- Properties and applications of mammalian OBPs. Figure was based on Gonçalves et al. (2021).

1.6.1. Biosensors

These proteins can be used to create devices capable of detecting a specific compound, to be applied in many different industries, including agriculture and food. The use of OBPs as biosensors becomes an advantage since, they are easier to synthesize and have a relatively lower cost compared to the alternatives in the market.

1.6.1.1. Medical diagnostics

Volatile organic compounds (VOCs) from the skin, respiratory and digestive channels, can give information about the diagnosis of diseases in modern medicine serving also for the biometric identification in forensic science (Sorokowska et al., 2016). Lu et al. (2016) developed an electrochemical biosensor containing a human recombinant OBP with a nanopore matrix to detect specific biomolecular ligands, such as aldehydes and fatty acids. The biosensor showed potential for the detection of odors and biomolecules for the diagnosis and evaluation of diseases.

1.6.1.2. Detection of hazard substances

The detection and identification of hazard substances, like explosives or drugs, is of great relevance specially for customs agencies (Giannoukos et al., 2016). Training animals to detect these substances is costly being necessary to find straightforward techniques to avoid the use of animals (Habib, 2007). A sort of analytic instruments is available for the detection of specific compounds in trace

quantities, for example mass spectrometers (MS), ion mobility spectrometers (IMS), handheld gas chromatographs (GC), Raman spectrometers, Surface enhanced Raman spectroscopy and “electronic noses” based on many different detection technologies (Zalewska et al., 2013). However, these instruments may present false positives, which is leading to the search of alternatives.

Cali & Persaud (2020) recently created a series of chemical sensors for drug detection based on a modified odorant-binding protein from *Anopheles gambiae*. The authors found that AgamOBP1_S82P has a high affinity for cannabinol, 3,4-methylenedioxy methamphetamine (MDMA / Ecstasy) and cocaine hydrochloride. Scorsone et al. (2021) also demonstrate that devices based in OBPs can detect a range of explosives and drugs with high sensitivity and selectivity. They studied the characterization of natural and expressed Ligand Binding Proteins, using molecular modeling and fluorescent displacement assays to select proteins based on ligand binding affinities of the target compounds to the protein binding pockets (Scorsone et al., 2021). In another study Cennamo et al. (2015), developed an optical biosensor based on pig OBP (pOBP), deposited on a plastic optical coupled with a surface plasmon resonance (SPR) transduction fiber for the detection of butanal. The price and detection range of this device is an asset as it has a reduced cost and allows a detection range between 20 and 1000 μM (Cennamo et al., 2015).

1.6.1.3. Food

Artificial olfactory systems, consisting of electronic nose devices (e-noses) have been created to mimic the sense of smell. The interaction of VOCs with the e-nose biosensor generates a signal (electrical, optical, or gravimetric), which is translated and processed by a signal processing computer (Zhang et al., 2018). The main application of these e-noses on food-processing industry (fish, meat, milk, wine, coffee and tea) is mainly related with the sensory evaluation of the products (Loutfi et al., 2015).

Di Pietrantonio et al. (2015) found that pOBP can also bind to octenol and carvone, which are VOCs associated with the presence of fungi and molds. They immobilized this protein, and the sensor was able to detect R-carvone (di Pietrantonio et al., 2015).

In another study, two peptides were extracted from the sequence of *Drosophila melanogaster* LUSH-OBP, due to its known sensitivity and selectivity for alcohols, to detect food contamination by Salmonella, since the main VOC released from meat contaminated with Salmonella is the 3- methyl-1-butanol (Sankaran et al., 2011).

The use of these e-noses in the food industry has reduced the difficulty and cost of industrial food processes.

1.6.1.4. Agriculture

OBPs are shown to be useful in the agricultural industry. The knowledge about these proteins in insects allows their manipulation and study and the development of high-performance insecticides (Leal (2013) . Liu et al., (2020) described the negative impact of *Diaphorina citri*, the main vector of the pathogen *Candidatus Liberibacter asiaticus*, on the citrus industry. In this study, the authors described the potential involvement of citOBP2 on the reduction of the insects' susceptibility to insecticides. The manipulation of DcitOBP2 might lead to the development of a new class of insecticides with great economic impact (Liu et al., 2020).

Latrophylline (LPH) participates in several essential physiological processes since it is a receptor coupled to the adhesion G protein. Xiong et al., were able to observe opposite changes in two chemoreception genes, chemosensory protein 10 (CSP10) and odorant-binding protein C01 (OBPC01), when the LPH knockdown in the insect under study. By silencing these two genes, they were able to observe that their susceptibility to dichlorvos or carbofuran increased, thus showing that the study of OBPs is useful in susceptibility to insecticides (Xiong et al., 2019).

1.6.2. Capture and release of odors

The detection capabilities of OBPs have opened doors to other areas such as odor capture and release. Since they can capture volatile odorants in the first events of olfactory perception, OBPs function as the first selective filter and can be good candidates of biotechnological interest to concentrate, discriminate or discard chemical compounds present in the air in traceable quantities, not physiologically perceived (Guiraudie-Capraz et al., 2005). Guiraudie-Capraz et al. (2005) described the use of substantial amounts of highly purified rOBP for the efficient screening of physiological odorants.

Gonçalves et al. (2018) fused pig OBP to three cell-penetrating peptides (CPPs), called Tat, Pep-1 and pVEC (**figure 8**), and when added to the liposomes, these new fusion proteins revealed different transduction efficiencies of a model ligand, 1-aminoanthracene (1-AMA), in liposomes (Gonçalves et al., 2018)

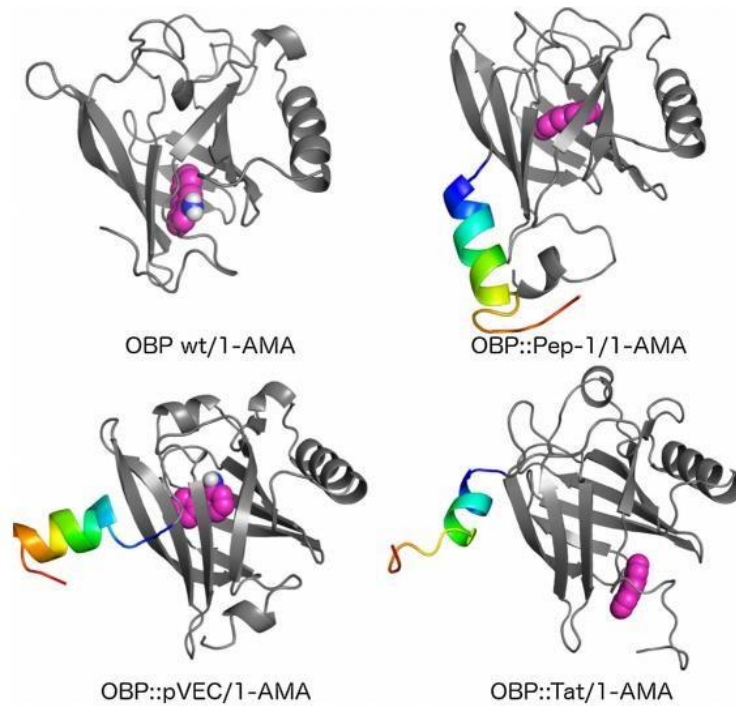


Figure 8- Pig OBPs fused to three cell-penetrating peptides. Figure taken from Gonçalves et al. (2018).

In another study, Gonçalves et al. (2018), evaluated the effect of the proximity of OBPs to the liposome membrane on the transduction of 1-aminoanthracene (1-AMA) (**figure 9**). The anchoring of the porcine odorant-binding protein (OBP-I) onto the liposomal membrane was promoted by the peptide SP-DS3 fused to OBP-I. The anchoring capacity and the proximity effect were confirmed by an experimental control where the wild type (wt) OBP was added to the liposomes, resulting in low 1-AMA transduction and low binding to OBPwt (Gonçalves et al., 2018).

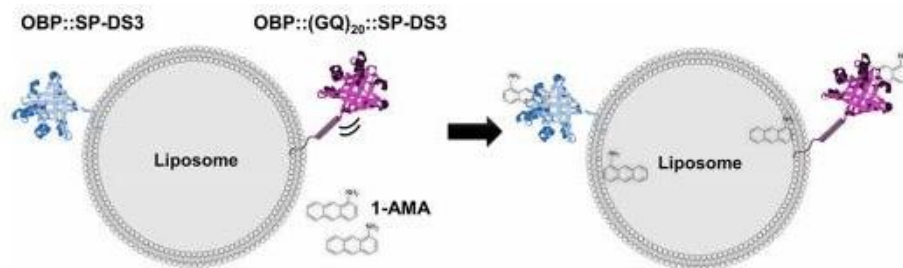


Figure 9- Representation of an anchorage-based system composed by fusion OBPs and liposomes for the entrapment and transport of molecules. Figure taken from Gonçalves et al. (2018).

In Gonçalves et al. (2018) the authors designed two proteins based on the OBP-I sequence: truncated OBP (tOBP) and OBP: GQ20: SP-DS3 and tested the binding affinity of 1-AMA to these proteins. They concluded that this molecule showed different affinities to temperature (**figure 10**) and described for the first time a temperature-dependent competitive mechanism for this class of proteins ((Gonçalves et al., 2018). These works paved the way to explore new strategies for the release and capture of odors.

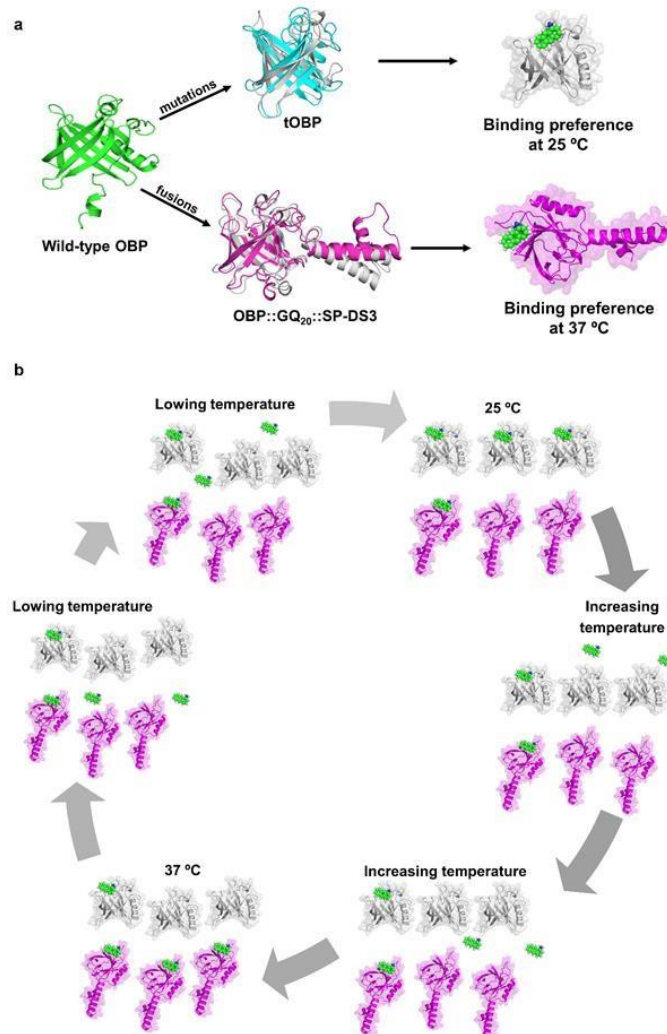


Figure 10- Opposite temperature-dependent affinities of tOBP and OBP:GQ20: SP-DS3 to 1-aminoanthracene (1-AMA). (a) Different binding affinities of tOBP and OBP:GQ20: SP- S3 (b) OBP's competitive temperature-dependent mechanism. Figure taken from (Gonçalves et al., 2018).

1.6.3. Textile industry

The use of textiles in several areas has been increasingly recurrent with the advancement of science and technology. More and more techniques have emerged that allow the attribution of different properties not previously possessed by textiles. Among the textiles' functionalization techniques are included physical, chemical nano and bio technologies (Huang et al., 2012).

Textiles attract, adsorb and store various gaseous compounds from their surroundings. The control of odors can be accomplished by capturing substances with unpleasant smells and by releasing fragrances. To counter bad odors and incorporate lasting fragrances into textiles, several studies were carried out using OBPs.

Silva et al. (2014) cloned and expressed a pig OBP gene in *E. coli* to explore the application of this protein on odor control and fragrance delayed release from a textile surface. They observed a strong binding of citronellyl valerate, citronellol and benzyl benzoate to the recombinant protein, while ethyl valerate displayed weaker binding. They coated cationized cotton substrates with porcine OBP and tested their ability to retain citronellol and mask the smell of cigarette smoke. It was possible to observe that the immobilized protein delayed the release of citronellol when compared to untreated cotton and through a blind evaluation of 30 evaluators, there was observed a decrease in the smell of cigarette smoke on the fabric surface due to the incorporation of the pig OBP. This study also demonstrated that the pig OBP can be an efficient solution to prevent and/or remove unpleasant odors trapped on the large surface of textiles (Silva et al., 2014).

In another study, Goncalves et al. (2019) described the effect of saline solutions (artificial sweat, pH 4.3-8.5) on the release of a fragrance, β -citronellol, from pOBP-functionalized cotton. Taking advantage of OBP response to sweat triggering ($<K_a$) the authors developed a smart responsive OBP-functionalized textile. They observed that when in contact with a sweat solution, the fragrance was released from the OBP at the cotton surface (**figure 11**). This study opened new opportunities for the development of devices that generate a response to odors of daily activities and physical exercises.

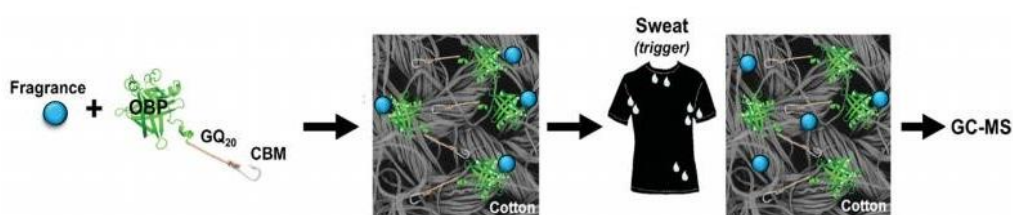


Figure 11- Release of fragrance from OBP-functionalized cotton, triggered by sweat. The release of fragrance was measured by GC-MS. The figure was taken from Goncalves et al. (2019).

1.7. Challenges

Although the mechanisms of interaction between the OBP and ligands, and the OBP/ligand complex with the ORs are not yet well understood, it has been proven that OBPs contribute to olfactory perception at various levels: transport, prevention of oxidative stress and prevention of saturation of ORs (Silva et al., 2014; Wang et al., 2021). It is important to understand the interaction between OBPs and the ligands and how the complex OBP/ligand interacts with the OR.

There is a need to facilitate and improve the quality of human life and these proteins can be present in several areas such as the development of pollution detection devices, biosensors in agriculture, health and safety, cosmetic and food industry due to their great stability to thermal denaturation, pH and proteolytic degradation. (Gonçalves et al., 2021; Loutfi et al., 2015; Xiong et al., 2019).

In textile industry, although there are already studies regarding the application of these proteins (Goncalves et al., 2019), there is still a great difficulty in having proteins with greater binding capacity to cotton and polyester. As such, in the future, with technological advances, new applications and improvements are expected to emerge.

There is a large amount of information available about OBP structure and affinity to different molecules, allowing the design of specific mutants with tailored characteristics, representing a solid basis for customizing OBPs for different applications (Pelosi et al., 2014; Gonçalves et al., 2021).

2. AIMS

Due to daily activity and physical exercise, human beings sweat, resulting in unpleasant odors that cause social unrest and embarrassment. In order to counter this problem, the need arises to create functional textiles that incorporate fragrances that can be an effective clothing deodorant product. Several studies reveal that odorant binding proteins can capture and release odorant molecules when a specific trigger is present (Goncalves et al., 2019). Due to the large information regarding OBPs structure and affinity to different molecules it is possible the design of specific mutants with tailored characteristics.

This work is focused on the design, expression, purification and characterization of three different OBPs (designated by OBP 1, OBP 2 and OBP 3 due to confidentiality purposes), from pig OBP (PDB code 1A3Y), for the functionalization of textile substrates (cotton and polyester). These proteins will be expressed in an *Escherichia coli* strain (*E. coli* BL21(DE3)) and optimized for the best culture medium and growth temperature. After purification, they will be characterized alongside with OBP wild type (wt) in terms of size, purity (SDS-PAGE, MALDI-TOF) and structure (FTIR and DC). Afterwards binding assays will be performed with a model molecule (1-AMA) and competition assays with different fragrances will be conducted aiming to evaluate the ability of OBPs to bind these fragrances. The functionalization of textiles with the OBP/fragrance complex will be evaluated under two different methods: impregnation and spray. Fragrance release from OBP functionalized textiles will be studied under different temperatures.

3. MATERIALS AND METHODS

3.1. Expression of OBPs

The expression of the OBP proteins started by transforming an *E. coli* BL21 (DE3) strain and test different medium and temperature conditions to find the best production conditions.

3.1.1. Transformation of *E. coli* BL21 (DE3) strain

E. coli BL21 (DE3) cells were transformed through the Transformation and Storage Solution Method (TSS Method). This method combines two steps of a classic transformation protocol aiming the production and transformation of competent cells only one stage. The TSS solution is composed by Lysogeny broth (LB) (Grisp, Portugal) with 10% (w/v) PEG Mw 3350, 5% (v/v) DMSO and 50 mM of MgCL2 (Chung et al., 1989). The cells were grown in LB medium until reach an OD600 between 0.3 - 0.4. The cells were centrifuged and then resuspended in TSS solution.

These competent cells were then transformed with the pET-28 a (+) vectors with the OBP genes (GenScript (USA).) For this, 1 μ L of the vector containing the gene of interest was added to the cells. The cells were incubated for 30 min on ice followed by a thermal shock at 42 °C, for 2 minutes and then incubated 2 minutes on ice. LB medium pre-heated at 37 °C was added to the cells followed by an incubation at 37 °C, 200 rpm for 1h. Afterwards, the cells were plated (100 μ L, 250 μ L and 650 μ L) on LB-Agar, supplemented with kanamycin (0.05 mg/mL) (Fisher Chemical), and incubated at 37 °C for 16 hours. The number of colonies were counted and a screening of protein expression was performed (Seidman et al., 2001). The efficiency of the transformation was calculated using the **equation 1**.

$$\text{Efficiency} = \frac{\text{number of colonies}}{\text{volume (L)}} \times 10^{-5} \text{ UFC}/\mu\text{gDNA} \quad \text{(Equation 1)}$$

This protocol was replicated for the 3 proteins, OBP 1, OBP 2 and OBP 3.

Sodium dodecyl sulfate-polyacrylamide gel electrophoresis (SDS-PAGE), running gel of 12.5% and staking gel of 4%, were performed to determinate the molecular weight of OBP proteins. In **table 1**, it is present the theoretical molecular weight of each OBP protein.

Table 1- Theoretical molecular weight of each protein.

Protein	OBP 1	OBP 2	OBP 3
Molecular weight (kDa)	24.8	22.9	25.8

3.1.2. Screening of protein expression

For the screening of OBPs expression, eight colonies of each transformant (OBP 1, OBP 2 and OBP 3) were selected. A pre-inoculum of four transformants of each protein were prepared by growing the transformants in LB medium supplemented with kanamycin (0.05 mg/mL) at 37 °C and 200 rpm, overnight. After this period of incubation, the OD₆₀₀ of each transformant suspension was measured. The volume of pre-inoculum necessary was calculated using **Equation 2** to provide a final OD of 0.1 in 10 mL of TB- AIM medium supplemented with kanamycin (0.05 mg/mL) and incubated for 24 h at 37 °C.

$$\text{Initial Volume} \times \text{Initial OD} = \text{Final Volume} \times \text{Final OD} \quad (\text{Equation 2})$$

This process was repeated for each protein and at different fermentation temperatures (30 °C, 25 °C and 18 °C). The samples were analyzed by Sodium dodecyl sulfate-polyacrylamide gel electrophoresis (SDS-PAGE) to infer the best production conditions.

3.1.2.1. Sodium dodecyl sulfate-polyacrylamide gel electrophoresis (SDS-PAGE)

Sodium dodecyl sulfate-polyacrylamide gel electrophoresis (SDS-PAGE), running gel of 12.5% and stacking gel of 4% (**table 2**), were performed to evaluate the expression of the OBPs. The samples were prepared with 2x Sample Loading Buffers, followed a denaturation step at 100 °C for 5 min. The gel was loaded with the molecular weight marker (Grisp), GRS Protein Marker Blue and the OBP samples. The gel was ran (20 mA per gel), and stained with a Coomassie solution (methanol 50% (v/v), acetic acid 10% (v/v), Coomassie Brilliant Blue G-250 (2.5 g/L) for 15 min followed by a destaining step with warm distilled H₂O. SDS-PAGE staining with Coomassie Blue is an easy and inexpensive technique that allows us to perform a direct assessment of the purity of the sample.

Table 2- Composition of running and stacking gel in SDS-PAGE

SDS-PAGE	Running gel (12,5%) (mL)	Stacking gel (4%) (mL)
Acrylamide/Bis-acrylamide (30 %/0.8 %(w/v))	4,125	0,7
0.5 M Tris-HCl (pH 6.8)	-	1,3
1.5 M Tris-HCl (pH 8.8)	2,5	-
SDS (10%)	0,01	0,005
H₂O	3,22	2,92
TEMED	0,001	0,001
APS (10% (w/v))	0,0075	0,00375
Final Volume	10	5

3.1.3. OBPs production and purification

The production of the OBPs was done using the best expression conditions (TB medium supplemented with kanamycin (0.05 mg/mL) and incubated for 24 h at 200 rpm and 30 °C for OBP 1 and 25 °C for OBP 2) determined by SDS-PAGE. After expression, the cells were incubated for 1 h at 4 °C and then were harvested by centrifugation at 6000 rpm at 4 °C for 10 min, and resuspended in phosphate buffer (20 mM NaH₂PO₄, 500 mM NaCl, pH 7.4). The cells were further centrifugated at 6000 rpm at 4 °C for 10 min and resuspended in phosphate buffer supplemented with 20 mM of imidazole. After, the protease inhibitor was added to the solution and lysed by sonication or homogenization.

The cells were lysed by ultrasonication (amplitude of 40%; 3 seconds ON: 9 seconds OFF, with a total sonication time of 30 min) or by high pressure homogenization (1500 bar, 10 min). Afterwards, the cells were centrifugated at 6000 g for 10 min at 4 °C in order to separate the fractions and a SDS-PAGE was done in order to determinate if the OBPs were present in the soluble or insoluble fraction

The OBPs were purified through nickel magnetic beads with specificity to His-tag sequence present in the proteins' N-terminal. The samples were poured into the containers with the nickel magnetic beads and incubated for 1 h at 4 °C and 100 rpm. After the incubation the containers with the samples and the nickel magnetic beads were inverted several times and then it was performed a magnetic separation. The beads were washed with different concentrations of imidazole (30, 50, 70, 80 mM) and eluted with 100, 250 and 500 mM (3 times) of imidazole.

After purification, the proteins present in the different concentration of imidazole were dialyzed against distilled water for 4 days at 4 °C, to remove the presence of salts and imidazole. After 4 to 5 days the protein solution was poured into containers and freeze-dried. The protein weight was determined and the expression yield was calculated using **equation 3**.

$$\eta = \frac{\text{protein weight (mg)}}{\text{Culture media volume(L)}} \quad \text{(Equation 3)}$$

3.2. Characterization of OBPs

3.2.1. MALDI-TOF

To verify the mass/charge of OBPs a Matrix-Assisted Laser Desorption/Ionization with time-of-flight (MALDI-TOF) was carried out using sinapic acid (SA) as the matrix ($\geq 99.5\%$). Using an Ultra-flex MALDI-TOF mass spectrophotometer (Bruker Daltonics GmbH) equipped with a 337 nm nitrogen laser, the mass spectra were acquired. For the analysis of OBP proteins it was used a double layer deposition. The samples were previously dissolved in TA30 (30% acetonitrile/70% TFA), and mixed (1:1) with a saturated solution of SA in TA30. A volume of 2 mL of each mixture was spotted onto the ground steel target plate (Bruker part n° 209519) and analyzed using the reflective positive mode.

3.2.2. FITR

Fourier-Transform Infrared Spectroscopy (FTIR) was used to characterize the chemical structure of OBP proteins. The samples were placed directly on the crystal, and spectra were collected between 400 and 4000 cm^{-1} wavenumbers at a resolution of 2 cm^{-1} . Then, in the "Feat Peaks (Pro)" procedure of the "Peak Analyzer" menu in OriginPro software, v.8.5.0 (OriginLab Corporation, USA), the Convolved FTIR curves corresponding to the Amide I spectral interval of [1600; 1699] were analyzed. To identify discrete starting peak spectral locations for fitting it was done a Second Derivative built-in-method. Based on the provided peak assignments, the secondary conformational data arising from individual peaks were derived (Kong & Yu, 2007).

3.2.3. Circular Dichroism

The structural state of OBP proteins at different temperatures was evaluated by circular dichroism (CD) spectroscopy, using a Jasco J-1500 spectropolarimeter equipped with a temperature controller. CD spectra were recorded at 18 °C, 25 °C, 37 °C, 45 °C, 60 °C, 70 °C and 80 °C using a fixed concentration of 10 μM for each protein tested. It was also tested a spectrum at 80 °C with an incubation overnight at 4 °C to check the recovery of proteins' structure. The spectra were obtained over the wavelength interval of 180–260 nm at a scan speed of 10 nm/min and bandwidth of 1 nm. The path-length cell was 1 mm. Baseline was recorded at 25 °C with the same buffer of the samples (phosphate buffer, pH 7.5) and subtracted to the protein spectra. Final spectra were obtained by the average of three scans for each protein.

3.3. OBPs' Binding Performance

3.3.1. Ligand Binding Assays

The binding performance of the different OBP proteins was evaluated by direct titration with a ligand model, 1-aminoanthracene (1-AMA) as reported in Gonçalves et al. (2018). To determinate the optimal temperature of incubation for OBPs, the proteins were diluted in 50 mM Tris–HCl buffer pH 7.5, to a final concentration of 1 μM, and pre-incubated at 25 °C, 37 °C, 45 °C and 60 °C for 30 min. The ligand model, 1-AMA was dissolved in 95% ethanol at 2 mM and increasing concentrations of 1-AMA were added to a fixed concentration (1 μM) of each OBP and incubated at 37 °C for 1h.

The fluorescence of each OBP-ligand complex was recorded in a microplate spectrofluorometer with thermoregulation (BioTek Synergy MX) at 37 °C by increasing the emission intensity at 481 nm when excited at 295 nm. (Paolini et al., 1999; Eiríksdóttir et al., 2010; Silva et al., 2014)

The obtained data was fitted according to **equation 4** and the dissociation constants (Kd) were calculated using Graphpad by a non-linear regression method described in Malpeli et al. (1998). Y is the measured fluorescence ratio, [1-AMA]₀ is the initial concentration of 1-AMA and P₀ is the initial concentration of protein.

$$Y = \frac{[1-AMA]_0 + P_0 + Kd - \sqrt{([1-AMA]_0 + P_0 + Kd)^2 - 4P_0[1-AMA]_0}}{2P_0} \quad \text{(Equation 4)}$$

The corresponding association constant (K_a) was calculated using **equation 5**

$$K_a = 1/K_d \text{ (Equation 5)}$$

3.3.2. Competitive Binding Assays

A fluorescence competition experiment was carried out to determine the binding ability of the fragrances to OBPs. The binding capacity was evaluated as reported in Goncalves et al. (2019). For this, the OBPs were diluted in 50 mM Tris-HCl buffer, pH 7.5, to a final concentration of 1 μ M and pre-incubated at 25°C and 37°C for 30 min. Afterwards, the proteins were incubated with 2 μ M of 1-AMA at 37°C for 1h. Four fragrances, β -Citronellol (SAFC), (-)-Menthol (TCI), Eugenol (TCI) and Citronellil Valerate (SAFC), were tested. For this, 1, 2, 3, 10, 30 and 100 μ M of each fragrance were added to the previous solution (OBP+1-AMA) and incubated at 37 °C for 1h.

The emission fluorescence spectra were recorded on a microplate spectrofluorometer with thermoregulation (BioTek Synergy MX) at 37 °C by increase in the emission intensity at 481nm when excited at 295nm (Goncalves et al., 2019). The results were collected and using a non-linear fitting curve of OriginPro software, v.8.5.0 (OriginLab Corporation, USA) the fragrance concentration at which was observed a 50% decrease of 1-AMA fluorescence (IC50) was determined. The dissociation constant of each OBP protein was calculated by **equation 6** where K_{dF} is the dissociation constant of the fragrance, [1-AMA] is the fluorophore concentration used in the experiments (2 μ M), and k_{dPL} is the dissociation constant of the protein–ligand complex previously determined.

$$K_{dF} = \frac{IC50}{\left(1 + \frac{[1-AMA]}{K_{dPL}}\right)} \text{ (Equation 6)}$$

The association constant (K_a) was calculated as previously mentioned for the ligand binding assays.

3.4. Functionalization of textile substrates with OBP

3.4.1. Functionalization of textiles

Cotton and polyester fabrics were previously washed with a non-ionic detergent, Diadavin, according to ISO 105-C03-1978 standard, 50 °C for 60 min and then washed with tap water and distilled H₂O for 1 h. For the functionalization of the fabrics with the OBPs, two methods were tested i) impregnation and ii) spraying.

3.4.1.1. Method 1: Impregnation

In this method (**figure 12**) the cotton and polyester fabrics (2x2 cm²) were incubated with 100 μM of each OBP at different temperatures, 25°C, 37°C, 60 °C and 70 °C under 40 rpm for 2 h. The control experiments were performed by incubating the fabrics only with buffer (50 mM Tris-HCl pH 7.5). Afterward the fabrics were dried and incubated with a solution of 1% Coomassie Brilliant Blue at 60 °C for 1h, aiming to indirectly evaluate the amount of protein at the fabric's surface and infer the best operational temperature of incubation. The color strength was evaluated by means of K/S determination using a Color Reflectance Spectrophotometer, (Spectraflash 600 Plus CT from Datacolor International) coupled to a computer, at the maximum absorbance wavelength. The K/S analysis directly correlates the color intensity of the samples with the amount of protein at the surface after functionalization (Goncalves et al., 2019).

Once determined the best temperature of protein incubation the process was repeated using larger fabrics (5x5 cm²). The functionalized fabrics were left to dry and a square (1x1 cm²) of each was cut off. The rest of the fabrics were washed with 0,1% of Diadavin and once again a square (1x1 cm²) was cut off. This process was repeated for 3, 5, 10 and 20 washes. The same dyeing method and the percentage of color lost was determined, which thus determines the loss of protein impregnated on the polyester between washes.

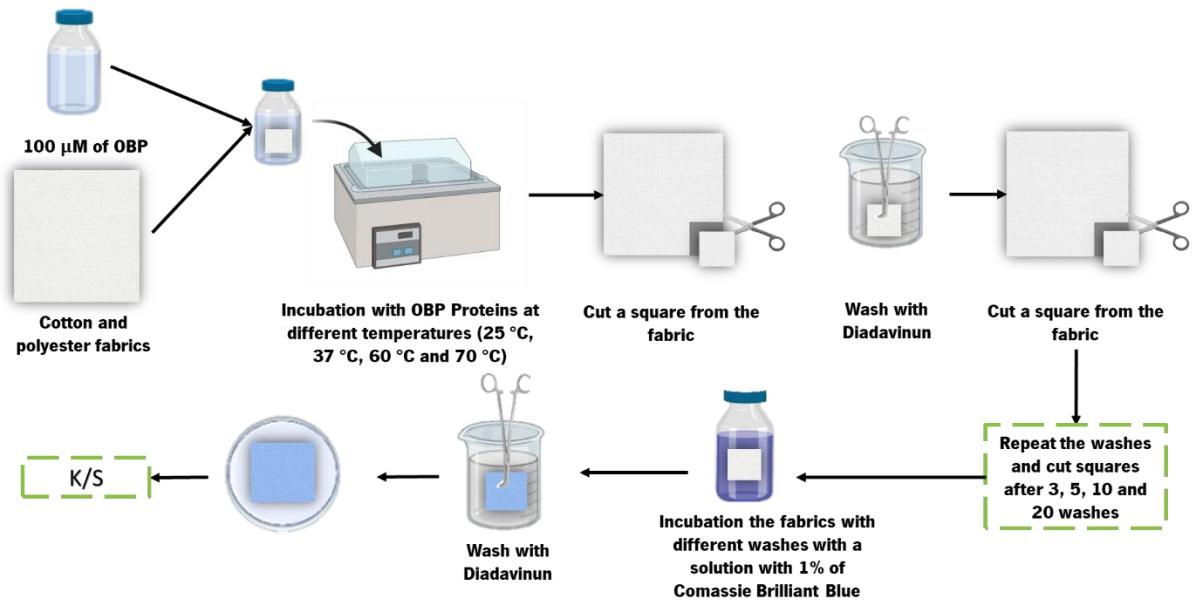


Figure 12- Functionalization of textiles by impregnation method.

3.4.1.2. Method 2: Spray

In this method (**figure 13**) polyester fabrics ($5 \times 5 \text{ cm}^2$) were incubated in a woven at different temperatures: 100 °C, 110 °C and 120 °C, for 1 h. Afterwards, each fabric was sprayed with a 1 mL solution of 100 μM of each OBP. The control experiments were performed by spraying the fabrics only with 1 mL of buffer (50 mM Tris-HCl pH 7.5). The fabrics were left to dry and a square ($1 \times 1 \text{ cm}^2$) was cut off. Then, the rest of the fabrics were washed with 50 mM Tris-HCl pH 7.5 and another square ($1 \times 1 \text{ cm}^2$) was cut off. This process was repeated for 3, 5, 10 and 20 washes.

All the fabrics were then incubated with a solution of 1% Coomassie Brilliant Blue at 60 °C for 1h, aiming to evaluate the protein loss during sequential washes. The K/S evaluation (color staining levels) was made with a Color Reflectance Spectrophotometer, (Spectraflash 600 Plus CT from Datacolor International) coupled to a computer, at maximum absorbance wavelength (Goncalves et al., 2019).

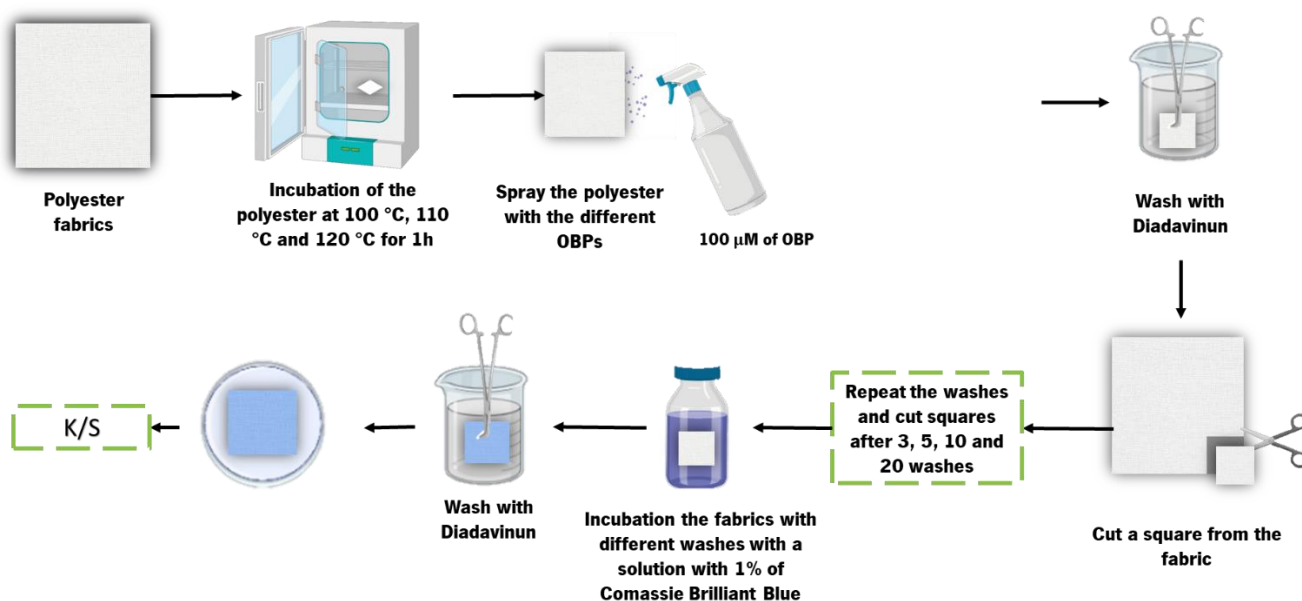


Figure 13- Functionalization of textiles by spray method.

3.4.2. Fragrance release from functionalized fabrics

The release of β -citronellol from functionalized fabrics (impregnation and spray methods) was evaluated according to the ISO 17299:2014 test standard procedure using the Gas Chromatography (Headspace SPME/GC-MS).

For the calibration curves, the SPME fiber was inserted in the middle (~40 mm from top) of the GC vial (22.5 × 75.5 mm, septa of silicone blue transparent/PTFE white, Enzymatic, Portugal) containing increasing concentrations of β -Citronellol (10-4000 μM). The fragrance was diluted using 50 mM Tris-HCl pH 7.5 prepared with distilled H₂O and the fiber was exposed for 2 and 4h. The amount of fragrance released was evaluated following the procedure described in section 3.4.2.4.

3.4.2.1. Complex Protein/fragrance

The functionalization of the polyester fabrics was carried out using the same two methods: impregnation and spray. The complex Protein/fragrance was obtained by incubating 100 μM of each OBP in a vial with 200 μM of β -Citronellol for 1h at 37°C. The 1:2 proportion (protein:fragrance) used was based on previous competitive assays.

3.4.2.2. Method 1: Impregnation

4 mL of the OBP protein/ β -Citronellol complex were transferred to a new vial containing the polyester fabric (1x1 cm²) and incubated for 2 h at 70 °C. After drying, the functionalized polyester was transfer to a GC vial followed by insertion of SPME fiber exposed for 2 h at 37 °C. The amount of fragrance released was evaluated following the procedure described in section 3.4.2.4.

3.4.2.3. Method 2: Spray

Polyester fabrics (1x1 cm²) were incubated at 120 °C for 1h and then sprayed with 2 mL of the OBP protein/ β -Citronellol complex. After drying, the functionalized polyester was transferred to a GC vial followed by insertion of SPME fiber exposed for 2 h at 37 °C. The amount of fragrance released was evaluated following the procedure described in section 3.4.2.4.

3.4.2.4. Quantification of β -Citronellol Release by Headspace- SPME/GC-MS.

The release of fragrance was evaluated via headspace (HS). The SPME fiber (100 μ m polydimethylsiloxane) was exposed to the vapor phase above the sample matrix, followed by gas chromatography–mass spectrometry (GC-MS) evaluation.

The samples were quantified by gas chromatography– mass spectrometry (GC-MS) using manual injection of the solid phase microextraction (SPME) fiber. The analysis was done using a Varian 4000 system with a split/splitless injector coupled to a mass spectrometer. Injections were operated at 250 °C in the split mode 1:10 using a Rxi-5Sil MS (Restek) column (30 m \times 0.25 mm, and 0.25 μ m film thickness), with a column-head pressure of 7.3 psi using helium as carrier gas. The oven temperature started at 45 °C and was held for 5 min, and the temperature increased until 250 °C at a rate of 7 °C/min. A full scan mode (50–750 m/z) was applied for the identification of the target compound. The mass spectrometer (MS) was operated in electron ionization (EI) mode at 70 eV with total ion chromatogram (TIC) detection mode for quantitative determination and S/N ratio of 5. Calibration curves of β -citronellol were determined using the same conditions of the samples (temperature and time). The β -citronellol released was determined integrating the peaks from chromatograms and quantified against the calibration curves using **equation 7**.

$$\% \beta\text{-Citronellol released} = \left(1 - \frac{([\beta\text{-Citronellol}]_t\text{-peak area})}{([\beta\text{-Citronellol}]_i)}\right) \times 100 \quad \text{Equation 7}$$

4. RESULTS AND DISCUSSION

4.1. Transformation of *E. coli* BL21 (DE3)

After transformation the number of colonies formed were counted and the transformation efficiency was calculated (**table 3**).

Table 3- Number of colonies and transformation efficiency of OBPs

Sequence	Number of colonies	Transformation Efficiency (UFC/ μ g DNA)
OBP 1	68	$6,8 \times 10^4$
OBP 2	163	$1,63 \times 10^5$
OBP 3	22	$2,2 \times 10^4$

4.1.1. Screening of protein expression

The different OBPs were incubated in TB-AIM medium at 37 °C and 200 rpm. The OBP 1 and OBP 2 were successfully expressed in these conditions (**figure 14 A and B**), however for the OBP 3, no expression was observed at 37 °C (**figure 14 C**). Even though OBP 3 showed no expression, the clone 2 was selected to verify if this protein could express using other temperatures.

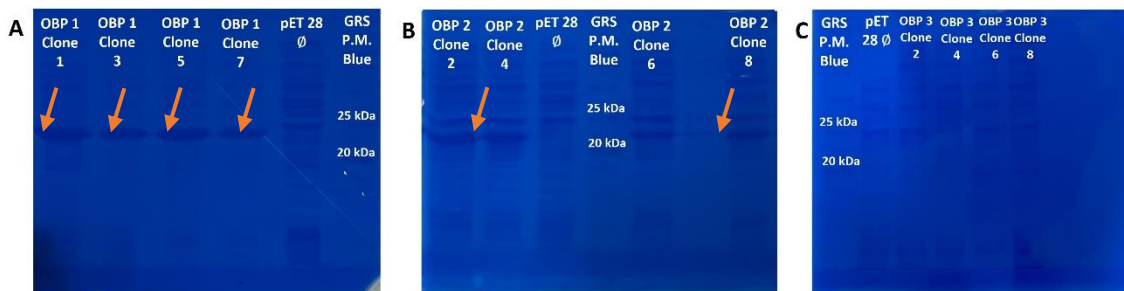


Figure 14- SDS-PAGE (12%) electrophoresis of different proteins expressed in TB-AIM at 37 °C, 200 rpm. (A) OBP 1 (B) OBP 2 (C) OBP 3.

Since OBP 1 and OBP 2 were expressed, the clones with better expression of each protein were selected to evaluate the best expression conditions. The clone 1 was selected for OBP 1, and the clone 2 for OBP 2.

The effect of incubation temperature on the protein expression was also evaluated (**figure 15**). Both OBP 1 and OBP 2 were expressed at 18 °C, 25 °C and 30 °C however OBP 3 was not expressed at any temperature (**figure 15 B**). In **figure 15 B** it is also possible to verify that, at 18 °C and 30 °C, OBP 2 shows a double band. Studies have pointed that pOBP such as bovine β -lactoglobuline, is dimeric at physiological pH, 7,2 (Albani, 2010; Burova et al., 1999). Considering the molecular weight of OBP 2 (22.9 kDa) the double band does not appear to represent a dimer, but rather a truncated version of the protein or another justification could be that protein degradation occurred during production or there was some translation problem during protein expression. The best conditions of expression were TB-AIM at 30°C for OBP 1 and TB-AIM at 25°C for OBP 2. **Table 4** presents a summary of the best expression conditions.

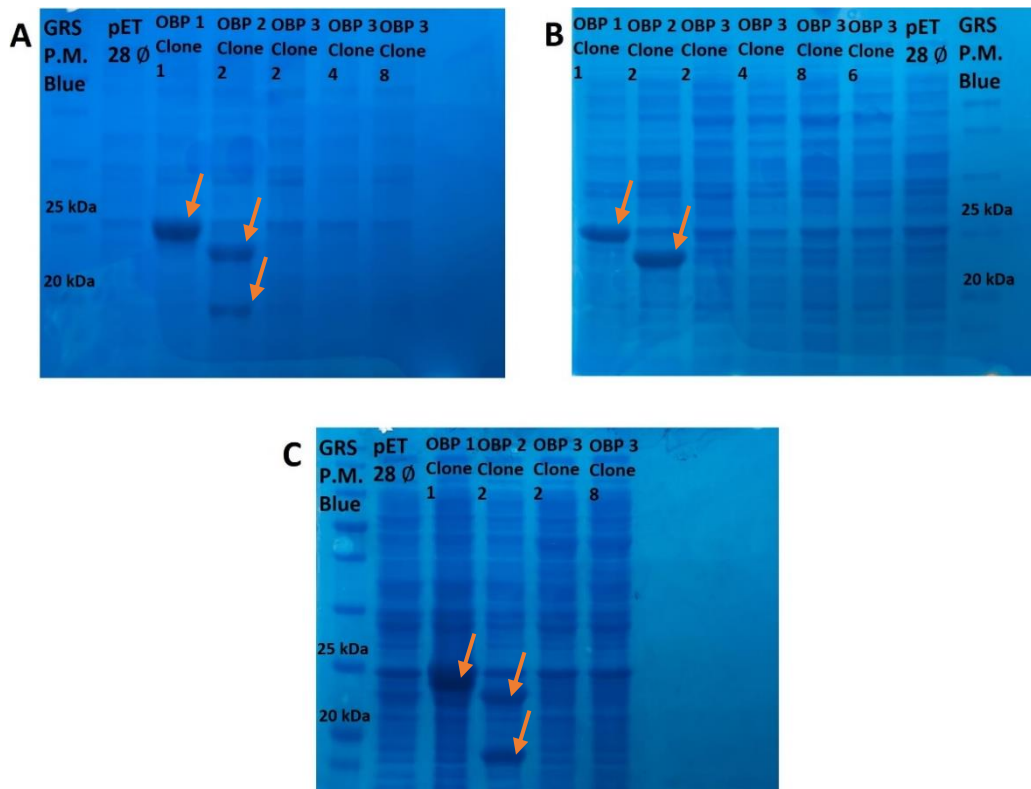


Figure 15- SDS-PAGE (12%) electrophoresis of OBP 1, OBP 2 and 3, incubated in TB-AIM at different temperatures and 200 rpm. (A) 30 °C (B) 25 °C (C) 18 °C.

Table 4- Cell culture medium and temperatures tested for the expression of OBP Proteins

Protein	OBP 1	OBP 2	OBP 3
TB-AIM (37 °C, 200 rpm)	✓	✓	-
TB-AIM (30 °C, 200 rpm)	✓	✓	-
TB-AIM (25 °C, 200 rpm)	✓	✓	-
TB-AIM (18 °C, 200 rpm)	✓	✓	-

4.2. OBP expression and purification

OBP 1 and OBP 2 were expressed in the best culture media conditions previously assessed: TB-AIM medium at 30 °C 200 rpm for 24 h for OBP 1 and TB-AIM medium at 25 °C, 200 rpm for 24 h for OBP 2.

After sonication the samples were analyzed by SDS-PAGE to evaluate if the proteins were in the soluble or insoluble fraction and both OBP proteins were in the soluble fraction (**figure 16**).

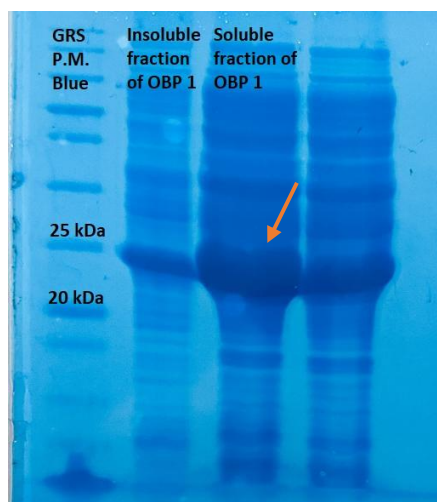


Figure 16- SDS-PAGE (12%) electrophoresis of the soluble or insoluble fraction of OBP 1.

4.2.1. Purification with nickel magnetic beads

To purify the samples, the soluble fractions were incubated with nickel magnetic beads for 1 h at 4°C, 100 rpm. After this period of incubation, the proteins of interest were eluted with increasing concentrations of imidazole (**figure 17**).

The SDS-PAGE revealed that OBP 1 was almost pure in the 70 mM imidazole fraction (**figure 15 A**) and OBP 2 in the 80 mM imidazole fraction (**figure 17 B**).

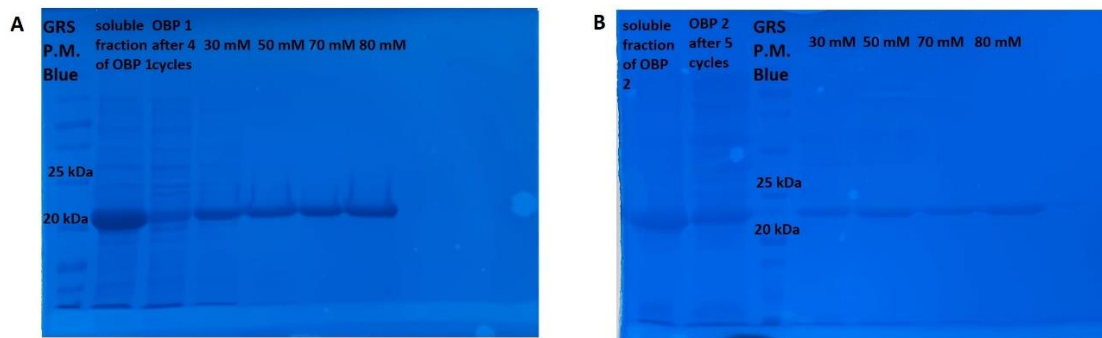


Figure 17- SDS-PAGE (12%) electrophoresis of: A) OBP 1 purified with nickel magnetic beads and eluted with increasing imidazole concentrations; B) OBP 2 purified with nickel magnetic beads and eluted with increasing imidazole concentrations.

4.2.2. Dialysis and Freeze drying

After 5 days of dialysis, the samples were freeze-dried (**figure 18 B**) and weighted to determine the yield of protein in mg per liter of culture media (**figure 18 A**).

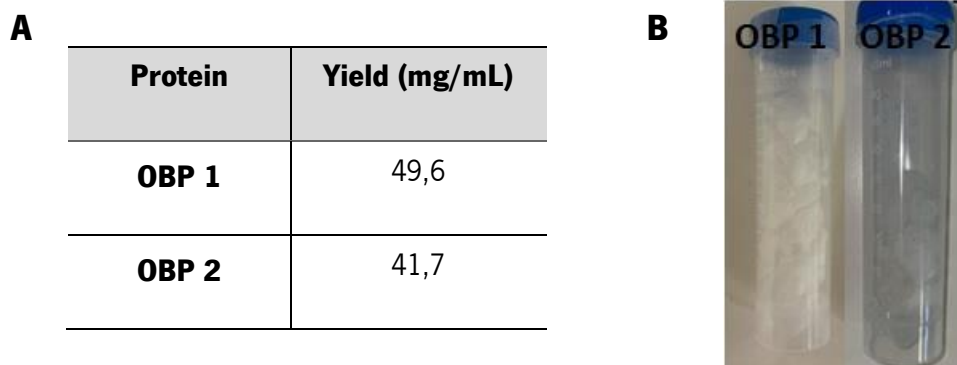


Figure 18- (A) Protein yield after purification (B) proteins after lyophilization.

4.3. Characterization of OBPs

4.3.1. MALDI-TOF

The molecular weight and purity of produced OBPs and OBP wt were assessed by SDS-PAGE electrophoresis (**figure 17**) and MALDI-TOF (**table 5**). The theoretical molecular weight of OBPs is similar to the experimental data obtained by MALDI-TOF, thus confirming the monodisperse character of the OBPs.

Table 5- Theoretical (by SnapGene® 3.0.3) and experimental (by MALDI-TOF) molecular weight of OBPs

Proteins	Theoretical Mw (kDa)	Experimental Mw (kDa)
OBPwt	20.2	20.1
OBP 1	24.3	26.5
OBP 2	22.9	-*

*Experimental determination was not possible due to ionization constrains during MALDI-TOF assessment.

4.3.2. FITR

The FTIR spectra of the 3 OBPs show the characteristics peaks corresponding to the amide I at 1630 cm^{-1} (**figure 19**).

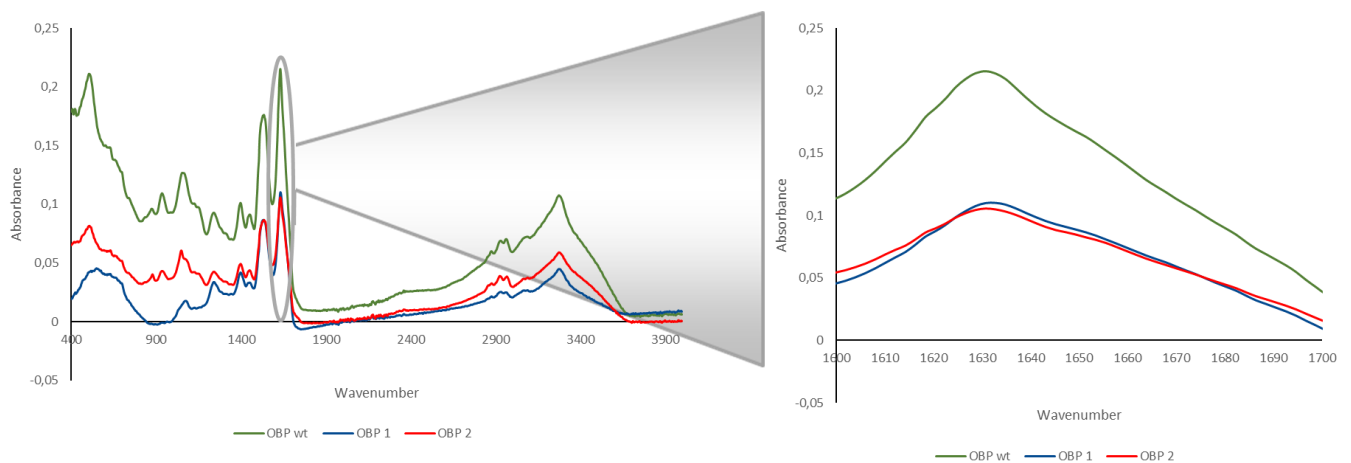


Figure 19- FTIR spectra of the OBP wt, OBP 1 and OBP 2 at amide I peak (1600- 1700 cm^{-1}).

After deconvolution of the amide I peak (**figure 19**) is possible to infer the secondary structure of each OBP (KONG and YU, 2007). The deconvolution of the amide I peak of OBPs show 5 peaks corresponding to 4 different structures. OBP wt is mainly constituted by β -sheet (**table 5**) which agrees with the literature (Pelosi et al., 2014; Vogt & Carolina, 2005). OBP 1 and OBP 2 present structural differences in relation to OBP wt. These proteins are based on OBP wt however with some modifications on their amino acidic sequence. Despite the substantial decrease in the % of β -sheet, OBP 1 is formed mostly by β -sheet (66,4%). There is an increase on the % of α -helix compared to OBP wt (2,9% in OBP wt to 8,4% in OBP 1) and in OBP 1 β -turn structures are present (19,5%) (**table 6**). For OBP 2 the initial structure was changed completely. This protein showed a greater % of α -helix (79,7%) which is totally different from OBP wt structure (2,9% α -helix). This protein has a small amount of β -turn structures compared to OBP 1 (2,62% and 19,5%, respectively) (**table 6**). These structural differences can lead to differences in the binding capacity of the proteins to fragrances and ligand molecules, as well as to alter their behavior under different conditions like temperature.

Table 6- Resulting discrete peaks, their respective contribution to the overall FTIR-derived curves and the corresponding structural assignments of OBP proteins. Structural assignment was performed according to KONG and YU (2007)

Proteins	Deconvoluted data assignment (%)			
	Helical	β - sheet	β -turn	Random
OBPwt	2,9	91,9	0	3,7
OBP 1	8,4	66,4	19,5	4,0
OBP 2	79,7	17,1	2,62	0

4.3.3. Circular Dichroism

The effect of temperature on OBPs' structure was evaluated by circular dichroism (CD) spectroscopy. As part of the superfamily of lipocalins, the OBPs share the same folding pattern, an eight stranded β -barrel flanked by a α -helix at the C-terminal end of the polypeptide chain (Pelosi et al., 2014).

OBPs have a similar shape of spectra, where the minimum is found at 195 nm and the maximum at 215 nm (**figure 20**). These values are characteristic of a fold with a high content of β -sheets.

It is possible to observe that for OBP wt (**figure 20 A**), OBP 1 (**figure 20 B**) and OBP 2 (**figure 20 C**), the protein structure changes are only observed at temperatures above 60 °C. As stated by Ioannou et al. (2015), the greater the intensity of the spectral peaks, the higher the amount of the corresponding secondary structure type.

As it can be seen in **figure 20**, when the OBP proteins are incubated at 80 °C, their secondary structure denatures, however, this process proved to be reversible for both OBP 1 and OBP 2. An assay was carried out in which the proteins were incubated at 80 °C followed by an incubation at 4 °C overnight. In **figure 20 A** (dashed line) it is possible to notice that the OBP wt keeps its structure unaltered while OBP 1 (**figure 20 B** (dashed line)) and OBP 2 (**figure 20 C** (dashed line)) recovered their structures after the overnight incubation period. This property could be associated with their structure being different from OBP wt as shown in FTIR results. Sawyer & Kontopidis (2000) points to a greater ease in the refolding of b-lactoglobulin, which belongs to the lipocalin family, when it had a greater number of α -helices than in its native form.

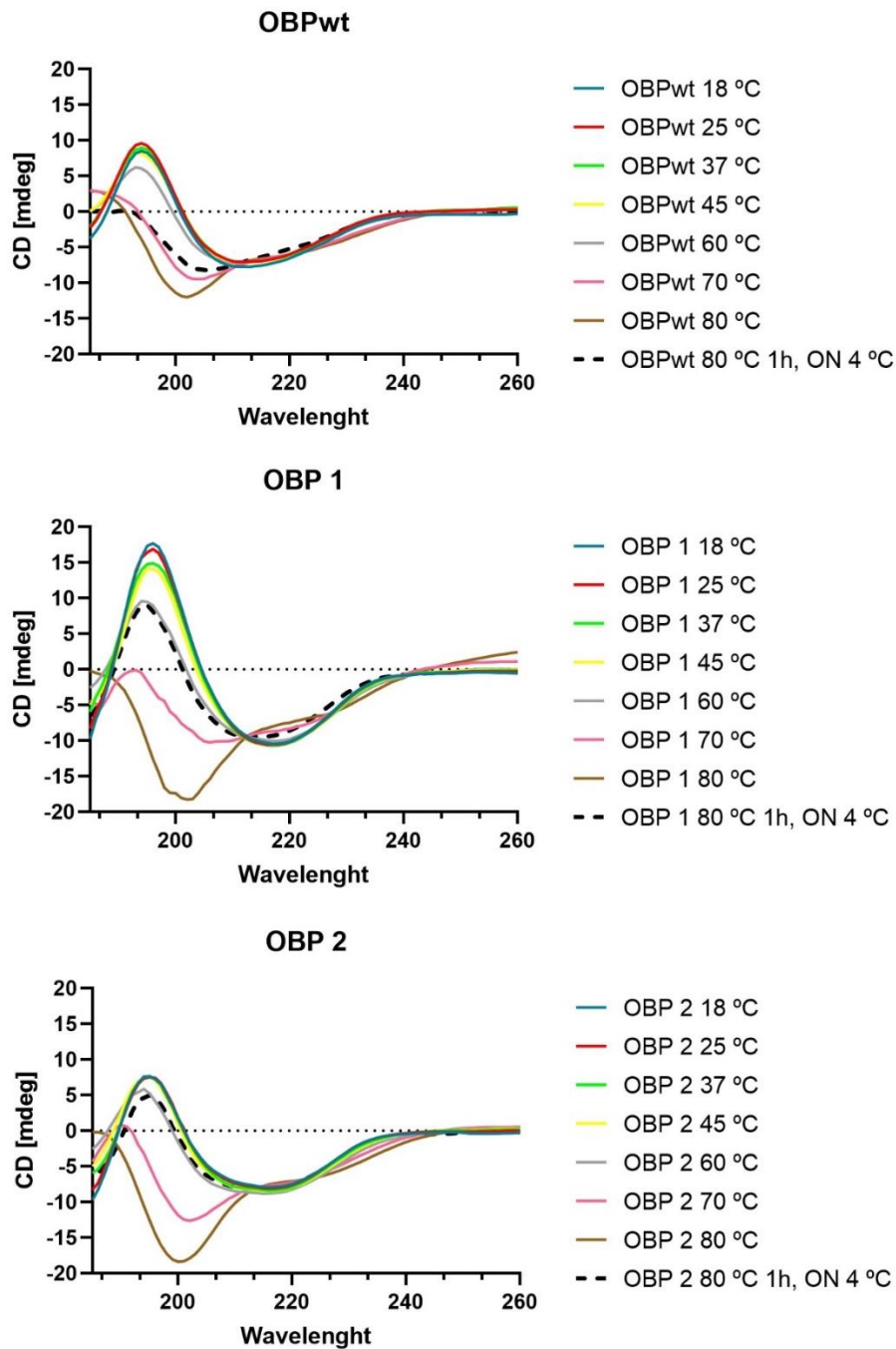


Figure 20- Circular Dichroism spectra of OBP wt, OBP 1, and OBP2. The spectra were obtained by inserting the data of each protein providing from Jasco J-1500 spectropolarimeter in GraphPad.

4.4. OBPs' Binding Performance

4.4.1. Ligand Binding Assays

Fluorescence binding assays were performed to test the binding capacity of the new OBPs to the ligand model, 1-AMA, at different temperatures after 1h of incubation at 37°C.

Paolini et al. (1999) showed that at a wavelength of 537 nm it is possible to monitor the free 1-AMA, while the binding of 1-AMA to OBP can be measured at 481 nm, since when the ligand model is bound at the binding site of OBP-I, the wavelength undergoes a small blue shift and the fluorescence intensity increases significantly.

The binding capacity was measured herein in terms of the dissociation constant (K_d). **Table 7** shows the results obtained being possible to notice for the three OPBs an increase on dissociation constant as the temperature increases. In Gonçalves, et al. (2018) fluorescence binding assays were also performed at a fixed concentration of protein and increasing concentrations of 1-AMA at 37°C for 1 h. For the OBP wt, they obtained a $K_d = 0.44$, which is in agreement with the result obtained by us for the OBP wt (Gonçalves, et al., 2018).

For all temperatures tested, it is possible to verify that the K_d of OBP 1 and OBP 2 is higher than that of OBP wt. The higher the K_d value, the lower the ability of proteins to bind the ligand. Therefore, OBP wt is the protein that binds best with 1-AMA at all the temperatures tested. These results point out the influence of extra amino acid sequence on 1-AMA affinity to the engineered OBPs, which resulted in a structural difference as can be confirmed by FTIR (**table 6**). Comparing both designed proteins, OBP 1 shows better affinity to 1-AMA than OBP 2 that can be attributed to differences on the protein structure (**table 7**). In **table 6**, it is possible to see that OBP 1 has a structure more similar to OBP wt (higher % of β - sheets) than OBP 2 which has a higher % α - helix than β - sheets, contrarily to OBP wt.

At higher temperatures (45 °C and 60°C) it is possible to verify that the K_d increases for all proteins, meaning that their binding ability to the model molecule, 1-AMA, decreases. The data obtained from the FTIR show that with increasing temperature, the 3 proteins lose their secondary structures. This can explain the decrease in the binding capacity of the ligand to the proteins.

Comparing the results obtained at different temperatures, it is possible to notice that for both OBP 1 and OBP 2, the best temperature of 1-AMA binding is 37 °C. In turn, the OBP wt presents better results at 25 °C. The competition tests will be carried out at 37 °C, since in general this was the best binding temperature of the model molecule.

Table 7- 1-AMA binding dissociation constants (Kd) of OBPs.

Protein	Kd			
	25 °C	37 °C	45 °C	60 °C
OBP wt	0,34	0,48	0,85	0,96
OBP 1	0,78	0,59	0,96	1,31
OBP 2	0,90	0,85	0,93	1,62

4.4.2. Competitive Binding Assays

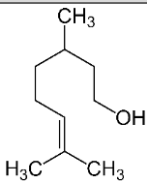
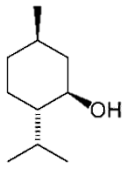
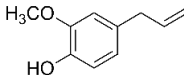
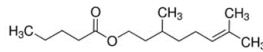
Fluorescence emission spectra were recorded at 37 °C with 2 μ M of 1-AMA in the presence of 1 μ M of protein, pH 7.5 for 1 h, followed by addition of increasing concentrations of β -Citronellol, (-)-Menthol, Eugenol and Citronellil Valerate, and incubated for 1 h at 37 °C. The proteins were pre-incubated at 25 °C and 37 °C for 30 min.

Previous studies show that there is a high affinity of the pOBP for the single-chain aliphatic molecules (e.g. citronellyl valerate) compared to shorter aliphatic molecules (e.g. citronellol) and to unsubstituted aromatic molecules (e.g. benzyl benzoate) (Silva et al., 2014). Four fragrances (β -Citronellol, (-)-Menthol, Eugenol and Citronellil Valerate) were selected based on the previous studied binding properties of OBP (**table 8**).

Table 8 shows the results obtained for the binding of different odorant molecules to OBPs as well as the differences observed depending on the pre-incubation temperature. Although being described in literature a higher affinity for the single-chain aliphatic molecules compared to shorter aliphatic molecules, our results demonstrate that, OBP wt as well as OBP 1 and OBP 2, displayed higher affinity for β -Citronellol.

OBP wt showed high binding to all fragrances tested but the best binding results were obtained for β -Citronellol (Kd=0,30) and (-)-Methol (Kd=0,30) when pre-incubated at 25 °C and for (-)-Methol (Kd=0.29) when pre-incubated at 37 °C. OBP 1 showed higher binding results for Eugenol (kD=0.30) and β -Citronellol (Kd=0.35) when pre-incubated at 37 °C. OBP 2 had higher binding affinity for β -Citronellol (Kd=0.29) when pre-incubated at 25 °C (**table 8**). These data make possible to infer that, in general, the highest binding results are achieved for β -Citronellol when the proteins are pre-incubated at 25 °C (room temperature).

Table 8- OBP-Fragrance dissociation constants (Kd)

Protein	Temperature	Kd			
		β -Citronellol	(-)-Menthol	Eugenol	Citronellil Valerate
					
OBP wt	25 °C	0,30	0,30	0,33	0,35
	37 °C	0,41	0,29	0,57	0,57
OBP 1	25 °C	0,61	0,62	0,61	0,65
	37 °C	0,35	0,59	0,30	0,53
OBP 2	25 °C	0,29	0,55	0,54	0,88
	37 °C	0,36	0,85	0,54	0,82

4.5. Functionalization of textile substrates with OBPs

4.5.1. Functionalization of fabrics

In this work, two methods were proposed for the functionalization of fabrics with OBPs. In the first method (Impregnation), polyester and cotton fabrics were incubated with 100 μ M of each OBP for 2 h at different temperatures, 25 °C, 37 °C, 60 °C and 70 °C. Then, the fabrics were stained with a 1% solution of Coomassie Brilliant Blue to infer the amount of protein at fabrics' surface. The color strength (K/S) directly correlates the color intensity of the samples with the amount of protein at the surface after functionalization, that is, the higher the K/S value, the greater the amount of protein on the surface of the fabrics.

For both cotton and polyester fabrics when functionalized with OBP wt and OBP 2, higher levels of functionalization were obtained at 70 °C (**figure 21**). For fabrics functionalized with OBP 1 the highest

levels of functionalization were obtained at 60 °C. Since the differences observed at 60 °C and 70 °C for this protein were minimal, 70 °C was considered as the best temperature condition for the functionalization of textiles by impregnation for the three OBPs. It was also possible to notice that an increase in textile functionalization with temperature.

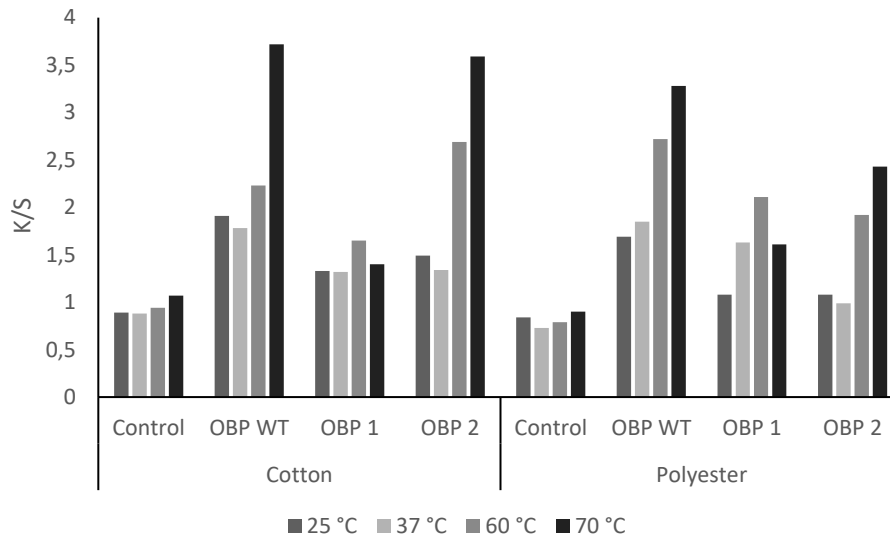


Figure 21- K/S evaluation of fabrics functionalized with OBPs using method 1 (Impregnation). Control samples were done with the fabric without any functionalization.

After determination of the best functionalization conditions, the process was repeated using larger fabrics (5x5 cm²) and sequential washes were performed to evaluate the fastness to washing of the functionalized fabrics. A piece of the fabric (1x1 cm²) was cut and stained with a 1% solution of Coomassie Brilliant Blue after 1, 3, 5, 10 and 20 washes of the main initial fabric. The K/S evaluation was performed, and **figure 22** shows the results obtained. Analyzing the results of functionalized fabrics without washes, it can be noted that OBP wt and OBP 1 present the highest K/S values, indicating a higher amount of protein coated onto the fabric. **Figure 22** shows that the K/S values decrease substantially after the first wash, especially for OBP wt and OBP 1. For OBP 2, the decrease is not so significant since the values without washing were already low meaning that lower amount of protein was coated onto the fabrics.

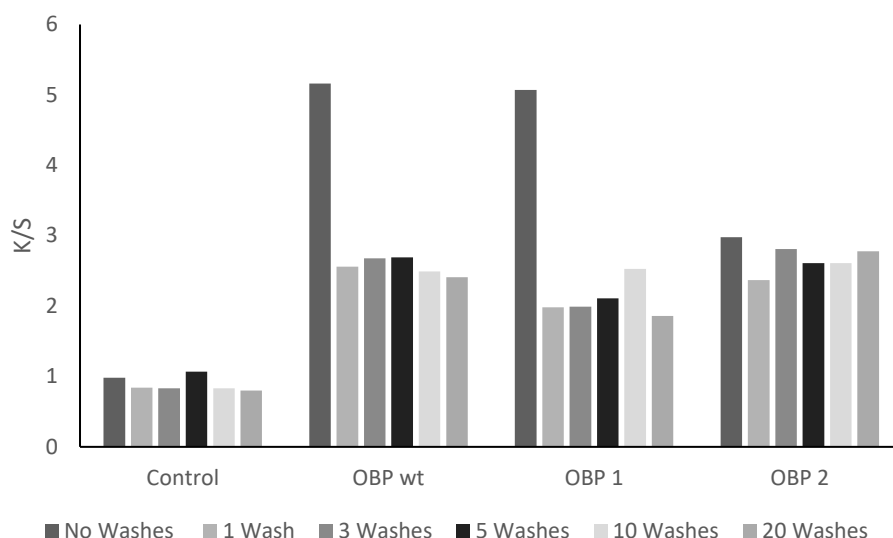


Figure 22- K/S evaluation of polyester fabrics functionalized using method 1 (Impregnation) with OBPs before and after 1, 3, 5, 10 and 20 washes. Control samples were done with the fabric without any functionalization.

The second method of functionalization (spray) consisted in the pre-incubation of the polyester fabrics at different temperatures, 100 °C, 110 °C and 120 °C and then spraying of 1mL solution of 100 μ M of each complex protein/fragrance onto these fabrics. Several washes were performed after spraying to evaluate the fastness to wash of functionalized samples. A staining with a solution of 1% Coomassie Brilliant Blue was performed followed by K/S (color staining levels) evaluation.

The best pre-incubation temperature differs depending on the OBP tested. For OBP 1, incubation at 100 °C resulted in a better functionalization, while for OBP wt and OBP 2, the best pre- incubation temperature was 120 °C. Overall, OBP 1 functionalized at 100 °C presented the highest K/S of all.

For this method, the resistance to washing was also evaluated (**figure 23**), which is important for domestic applications since the objective is for the textiles to remain functional for the highest number of washes. For the 3 OBPs, it is possible to notice that with the number of washes the values of K/S decrease until reaching a plateau. This indicates that the protein coated at the surface of the fabrics is removed by washing but a certain amount remains after 20 washes. Nevertheless, the best incubation temperature proved to be 120 °C, since the decrease of K/S values was less pronounced for samples pre-incubated at this temperature.

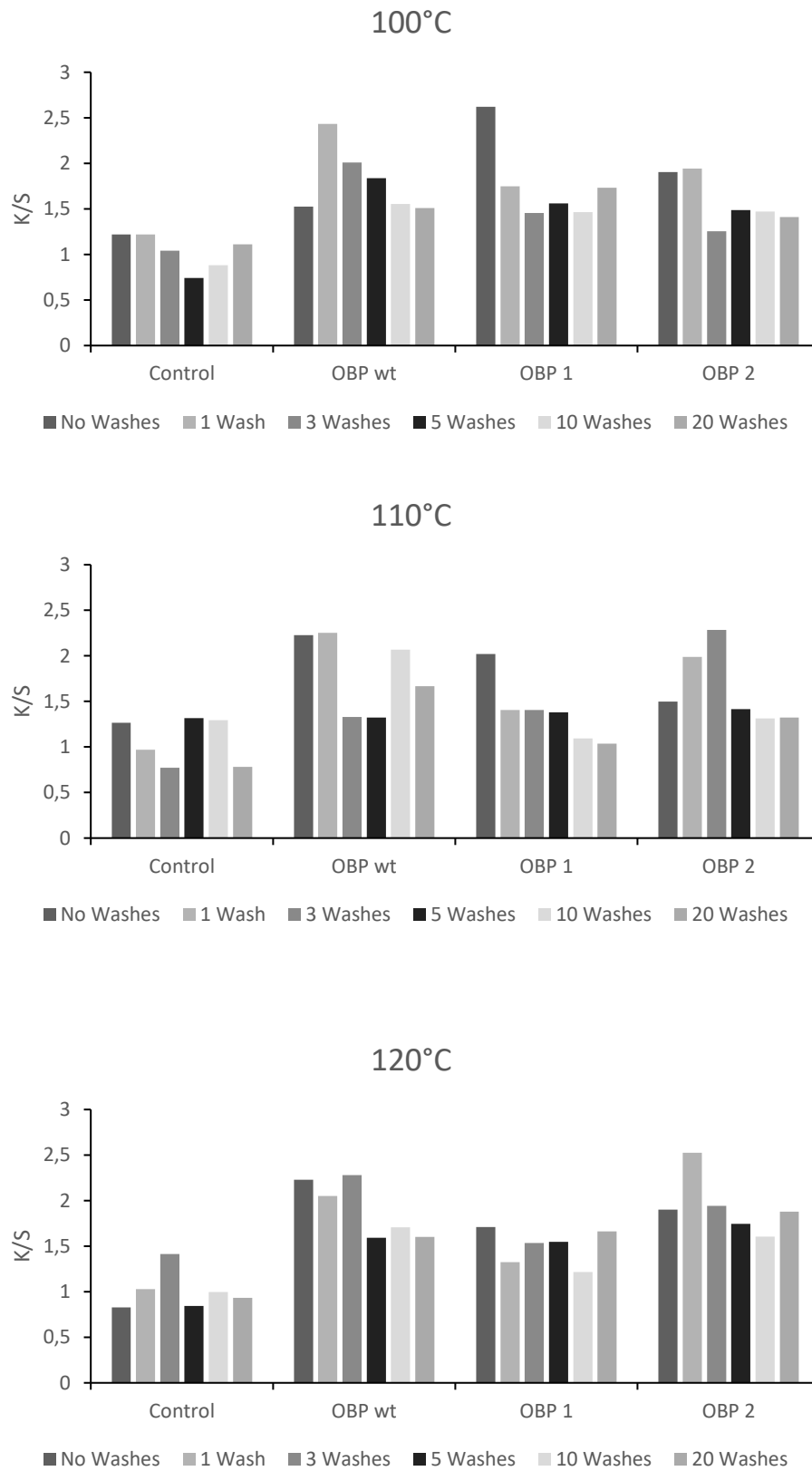


Figure 23– K/S evaluation of polyester fabrics functionalized with OBPs at different temperatures using method 2 (Spraying) and after different washes. Control samples were done with the fabric without any functionalization.

Comparing both methods of functionalization, impregnation and spray (**figure 24**), it is clear that the functionalization of polyester fabrics with the OBP wt through method 1 is the one that presents the highest k/s value, meaning a higher amount of protein was coated onto the fabrics. Through **figure 24** it is also possible to notice that for the three proteins, method 1 conferred the highest level of functionalization. After washing, there is a significant difference in the K/S value for OBP wt and OBP 1, whereas OBP 2 is more resistant to washing. In method 2, the difference in the K/S value during the washes was not so noticeable. This might be related with the initial lower amount of protein coated onto the fabrics when compared to method 1.

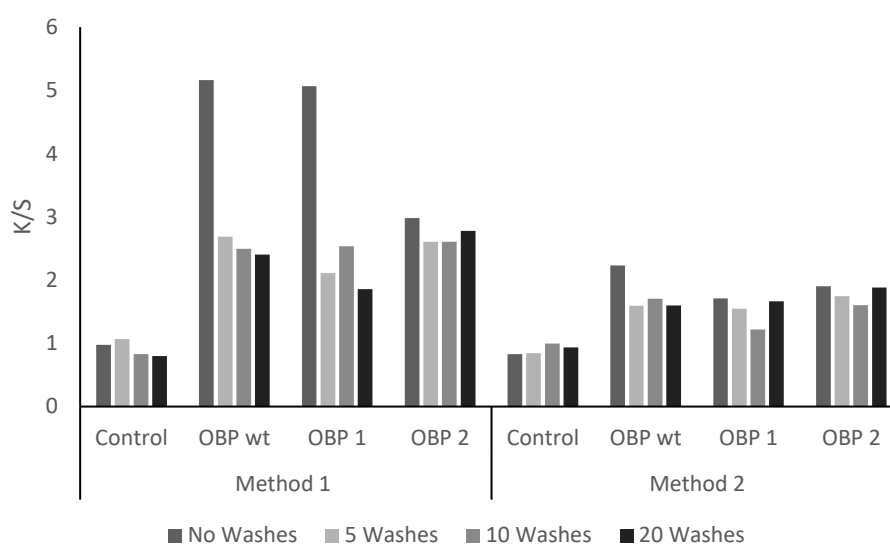


Figure 24- K/S evaluation of polyester fabrics functionalized with OBPs using method 1: impregnation at 70 °C and method 2: Spray at 120 °C and after different washes. Control samples were done with the fabric without any functionalization.

4.5.2. Evaluation of fragrance release from functionalized fabrics

The release of fragrance (β -citronellol) from functionalized fabrics was quantified by gas chromatography– mass spectrometry (GC-MS) using manual injection of the solid phase microextraction (SPME) fiber. The calibration curves were prepared using increasing concentrations of β -citronellol at the same conditions as the samples (**figure SI 1**) and each OBP protein was incubated with β -Citronellol for 1h at 37°C with a 1:2 ratio (protein:fragrance).

From the GC data (**figure SI 2, figure SI 3, figure SI 4 and figure SI 4**), a peak was obtained that corresponds to the mass spectra characteristics of β -citronellol with retention time of 16,7 min. The chromatograms of nonfunctionalized polyester did not reveal any peak.

For samples functionalized using method 1 (impregnation) the OBP/ β -Citronellol complex was transferred to a vial containing the polyester fabric (1x1 cm²) and incubated for 2 h at 70 °C. For samples functionalized using method 2 (spray) the fabrics were incubated at 120 °C for 1h and then sprayed with the OBP/ β -Citronellol complex. Afterwards, the functionalized polyester fabrics were transferred to a GC vial followed by insertion of SPME fiber exposed for 2 h at 37 °C. The β -citronellol released was determined integrating the peaks from chromatograms and quantified against the calibration curves.

Figure 25 compares the release of β -Citronellol for samples functionalized using both methods, before and after washing cycles. The results reveal a minimal release of the fragrance from samples functionalized with both methods, impregnation and spray. For samples functionalized using method 1, it is possible to observe the highest release of β -Citronellol from OBP wt on samples without washes. After washing the release decreases considerably as expected since, as previously described, a high amount of protein is removed from fabrics' surface by washing. For the 3 proteins tested, a similar behavior between washes is observed. As mentioned previously, the protein is removed from the fabrics' surface by washing until reaching a certain plateau where independently on the washing a certain amount of protein remains, which still contain fragrance to release when a temperature trigger is applied. For samples functionalized using method 2, the highest percentage of β -Citronellol released was observed for OBP 2, however a similar trend was observed after washes, an expressive decrease of fragrance release was observed immediately after the first wash. As previously described, the level of functionalization of OBP wt and OBP 1 was lower when using spray method, explaining the lower values of release obtained for these proteins before washing. After wash, both proteins followed the same trend observed for the other protein using the same method.

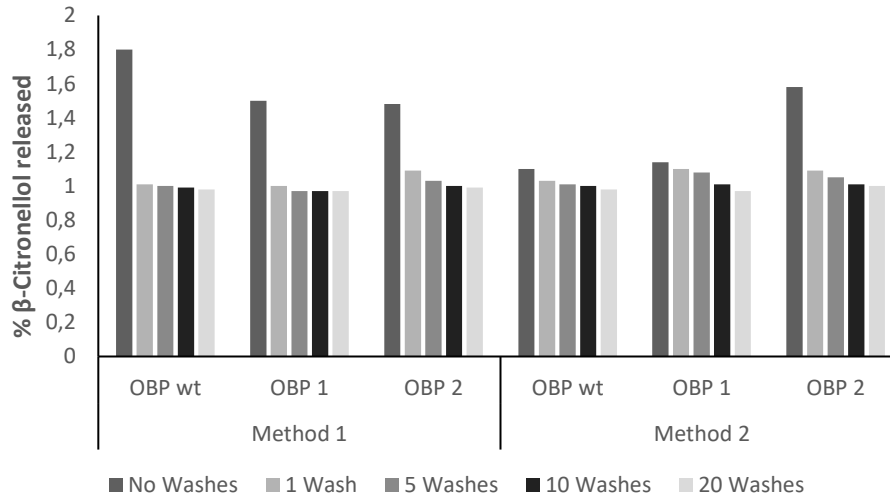


Figure 25- Evaluation of β -Citronellol release from OBPs after functionalization using method 1 (Impregnation) and method 2 (Spray), before washes and after washes.

Figure 26 shows the % of β -Citronellol loss between washes for both methods. For method 1, OBP wt has the highest loss of fragrance released between washes, while for method 2 the protein with the highest loss of fragrance between washes was OBP 2. This behavior was associated with the higher percentage of β -Citronellol initially released. These results are in agreement with those obtained in **figure 22**, since in both methods, the fabrics functionalized with the OBP/ β -Citronellol complex start by releasing different percentages of β -Citronellol and after 20 washes show a similar percentage of release.

It was also possible to notice the difference between the loss between method 1 and method 2 (**figure 26**). This difference is associated with the initial quantity of OBP/fragrance complex used in each method. Method 1 and method 2 starts with 100 mM of this complex. Prior to washing, it is not possible to determine the correct amount that remained on the fabrics. Quantification methods were done but there was a lot of interference because of the fibrils of the polyester fabric and that it was not possible to accurately determine the amount of protein that was placed at the beginning. After 20 washes the percentage of β -Citronellol released is under 1%, and for that it is not possible to determinate which method performed better.

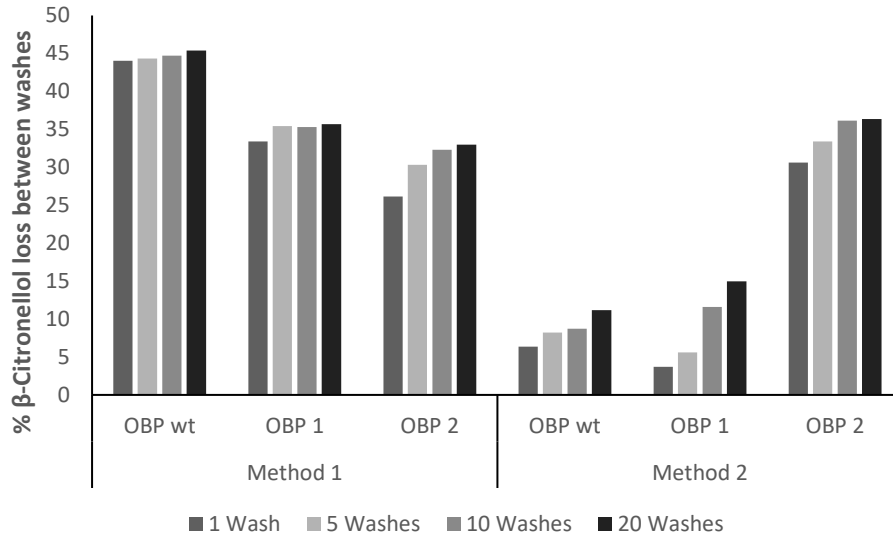


Figure 26- Evaluation of β -Citronellol lost between washes for samples functionalized using in method 1 (Impregnation) and method 2 (Spray).

5. CONCLUSION

This work aimed the design, expression, purification, and characterization of three different OBPs for the functionalization of textile substrates.

Several culture conditions were tested to find the best expression conditions for each OBP. OBP 1 and OBP 2 showed good expression levels for all the tested conditions, while for OBP 3 no expression was observed. The OBP 1 and OBP 2 were expressed in the best culture media conditions, TB-AIM medium at 30 °C 200 rpm for 24 h and TB-AIM medium at 25 °C, 200 rpm for 24 h, respectively. After sonication, the samples were analyzed by SDS-PAGE and was observed that the two proteins were expressed in the soluble fraction. The two proteins were obtained pure with a yield of 49,6 mg/mL for OBP 1 and 41,7 mg/mL for OBP 2.

After purification the OBPs were physico-chemically characterized by SDS-PAGE, MALDI-TOF, Circular Dichroism and FTIR. SDS-PAGE and MALDI-TOF data confirmed the molecular weight and the monodisperse character of OBP proteins. The deconvolution of amide I band from the FTIR spectrum revealed that OBP 1 and OBP 2 present variations on secondary structure when compared with OBP wt. Even though OBP1 is mainly composed by β -sheets the percentage of this comparing to OBP wt is must lower (OBP wt has 91,9% of β -sheets and OBP 1 66,4%). OBP 2, for instance, has a larger number of α -helix than β -sheets. These structural differences can lead to changes in the binding of proteins to fragrances and ligand molecules, as well as alter their behavior under different conditions such as temperature. The effect of temperature on OBP proteins was evaluated by circular dichroism spectroscopy. The three OBP proteins lost their structure for temperatures higher than 70 °C. However, when the OBP proteins were incubated at 80 °C (denaturation), this process proved to be reversible for both OBP 1 and OBP 2 after an incubation at 4 °C overnight. This property could be associated with their secondary structure being different from OBP wt.

The binding capacity of OBP proteins was evaluated by ligand and competitive binding assays. Fluorescence binding assays were performed at a fixed concentration of protein and increasing concentrations of a model ligand, 1-AMA and an incubation at 37°C for 1 h. The results show an increase of the dissociation constant when increasing the temperature. The competitive assays revealed that β -citronellol is the fragrance with the highest affinity towards OBP 1 and OBP 2.

In this work, two methods were proposed for the functionalization of textiles with OBP proteins. In the first method, polyester and cotton fabrics were incubated with 100 μ M of each OBP protein for 2 h at different temperatures. The second method consisted in the incubation of the polyester fabrics at

different temperatures and then spraying a solution with 100 μM of each protein on these fabrics. Several washes were performed at each temperature and for each protein. In both methods, was also performed a staining with a solution of 1% Coomassie Brilliant Blue and an evaluation of K/S (color staining levels) was done. For both cotton and polyester fabrics, the higher levels of functionalization were obtained at 70 °C in method 1 and for method 2, 120 °C is shown to be the best incubation temperature for the pre-heating treatment of the fabrics.

The release of fragrance was quantified by gas chromatography– mass spectrometry (GC-MS) using manual injection of the solid phase microextraction (SPME) fiber. The functionalization of the polyester fabrics was carried out using the impregnation and spray methods. Analyzing the GC-MS results, OBP wt has the higher % of β -Citronellol released after functionalization using method 1 and OBP 2 revealed the highest release when functionalized using method 2. Even though method 2 shows a smaller % β -Citronellol lost between washes, the method 1 shows higher % of β -Citronellol released. This difference is associated with the initial quantity of OBP/fragrance complex used in each method. Method 1 starts with 2 mL of this complex and method 2 with 1 mL. After 20 washes the percentage of β -Citronellol released is under 1%, and for that it is not possible to determinate which method performed better.

As these designed proteins showed properties different from the OBP wt, such as the possibility of recovering their structure after a period of incubation at high temperatures followed by an incubation at lower temperatures, they can be tested under other conditions. Other triggers can be applied to functionalized textiles such as different sweat pH, sweat ionic strength, abrasion and UV light or new functionalization methods can be tested in order to ensure that a greater amount of protein is retained on the surface of the fabrics and therefore in turn a greater release of fragrance from these.

6. REFERENCES

- Albani, J. R. (2010). Fluorescence properties of porcine odorant binding protein Trp 16 residue. *Journal of Luminescence*, *130*(11), 2166–2170. <https://doi.org/10.1016/j.jlumin.2010.06.013>
- Alfinito, E., Millithaler, J. F., Pennetta, C., & Reggiani, L. (2010). A single protein based nanobiosensor for odorant recognition. *Microelectronics Journal*, *41*(11), 718–722. <https://doi.org/10.1016/j.mejo.2010.07.006>
- Anderson, H. (1988). Drosophila adhesion molecules and neural development. *Trends in Neurosciences*, *11*(11), 472–475. [https://doi.org/10.1016/0166-2236\(88\)90002-1](https://doi.org/10.1016/0166-2236(88)90002-1)
- Archunan, G. (2018). *Open access Volume 14(1) Views Odorant Binding Proteins: a key player in the sense of smell*. <https://doi.org/10.6026/97320630014036>
- Barbosa, A. J. M., Oliveira, A. R., & Roque, A. C. A. (2018). Protein- and Peptide-Based Biosensors in Artificial Olfaction. In *Trends in Biotechnology* (Vol. 36, Issue 12, pp. 1244–1258). Elsevier Ltd. <https://doi.org/10.1016/j.tibtech.2018.07.004>
- Bignetti, E., Cavaggioni, A., Pelosi, P., Persuad, K. C., Sorbi, R. T., & Tirindelli, R. (1985). Purification and characterisation of an odorant-binding protein from cow nasal tissue. *European Journal of Biochemistry*, *149*(2), 227–231. <https://doi.org/10.1111/j.1432-1033.1985.tb08916.x>
- Boudjelal, M., Sivaprasadarao, A., & Findlay, J. B. C. (1996). Membrane receptor for odour-binding proteins. *Biochemical Journal*, *317*(1), 23–27. <https://doi.org/10.1042/bj3170023>
- Briand, L., Eloit, C., Nespoulous, C., Bézirard, V., Huet, J. C., Henry, C., Blon, F., Trotier, D., & Pernollet, J. C. (2002). Evidence of an odorant-binding protein in the human olfactory mucus: Location, structural characterization, and odorant-binding properties. *Biochemistry*, *41*(23), 7241–7252. <https://doi.org/10.1021/bi015916c>
- Brito, N. F., Moreira, M. F., & Melo, A. C. A. (2016). A look inside odorant-binding proteins in insect chemoreception. In *Journal of Insect Physiology* (Vol. 95, pp. 51–65). Elsevier Ltd. <https://doi.org/10.1016/j.jinsphys.2016.09.008>

- Buck, L., & Axel, R. (1991). A Novel Multigene Family May Encode Odorant Receptors: A Molecular Basis for Odor Recognition. In *Cell* (Vol. 65).
- Burova, T. v., Choiset, Y., Jankowski, C. K., & Haertlé, T. (1999). Conformational stability and binding properties of porcine odorant binding protein. *Biochemistry*, *38*(45), 15043–15051. <https://doi.org/10.1021/bi990769s>
- Cali, K., & Persaud, K. C. (2020). Modification of an *Anopheles gambiae* odorant binding protein to create an array of chemical sensors for detection of drugs. *Scientific Reports*, *10*(1), 1–13. <https://doi.org/10.1038/s41598-020-60824-7>
- Cennamo, N., Giovanni, S. di, Varriale, A., Staiano, M., di Pietrantonio, F., Notargiacomo, A., Zeni, L., & D'Auria, S. (2015). Easy to use plastic optical fiber-based biosensor for detection of butanal. *PLoS ONE*, *10*(3), 1–12. <https://doi.org/10.1371/journal.pone.0116770>
- di Pietrantonio, F., Benetti, M., Cannatà, D., Verona, E., Palla-Papavlu, A., Fernández-Pradas, J. M., Serra, P., Staiano, M., Varriale, A., & D'Auria, S. (2015). A surface acoustic wave bio-electronic nose for detection of volatile odorant molecules. *Biosensors and Bioelectronics*, *67*, 516–523. <https://doi.org/10.1016/j.bios.2014.09.027>
- Eiriksdóttir, E., Konate, K., Langel, Ü., Divita, G., & Deshayes, S. (2010). Secondary structure of cell-penetrating peptides controls membrane interaction and insertion. *Biochimica et Biophysica Acta - Biomembranes*, *1798*(6), 1119–1128. <https://doi.org/10.1016/j.bbamem.2010.03.005>
- Gaubert, A., Amigues, B., Spinelli, S., & Cambillau, C. (2020). Structure of odorant binding proteins and chemosensory proteins determined by X-ray crystallography. *Methods in Enzymology*, *642*, 151–167. <https://doi.org/10.1016/bs.mie.2020.04.070>
- Giannoukos, S., Brkić, B., Taylor, S., Marshall, A., & Verbeck, G. F. (2016). Chemical Sniffing Instrumentation for Security Applications. *Chemical Reviews*, *116*(14), 8146–8172. <https://doi.org/10.1021/acs.chemrev.6b00065>

- Gonçalves, F., Castro, T. G., Azoia, N. G., Ribeiro, A., Silva, C., & Cavaco-Paulo, A. (2018). Two Engineered OBPs with opposite temperature-dependent affinities towards 1-aminoanthracene. *Scientific Reports*, *8*(1), 1–12. <https://doi.org/10.1038/s41598-018-33085-8>
- Gonçalves, F., Castro, T. G., Nogueira, E., Pires, R., Silva, C., Ribeiro, A., & Cavaco-Paulo, A. (2018). OBP fused with cell-penetrating peptides promotes liposomal transduction. *Colloids and Surfaces B: Biointerfaces*, *161*, 645–653. <https://doi.org/10.1016/j.colsurfb.2017.11.026>
- Goncalves, F., Ribeiro, A., Silva, C., & Cavaco-Paulo, A. (2019). Release of Fragrances from Cotton Functionalized with Carbohydrate-Binding Module Proteins. *ACS Applied Materials and Interfaces*, *11*(31), 28499–28506. <https://doi.org/10.1021/acsami.9b08191>
- Gonçalves, F., Ribeiro, A., Silva, C., & Cavaco-Paulo, A. (2021). Biotechnological applications of mammalian odorant-binding proteins. *Critical Reviews in Biotechnology*, *40*(0), 1–22. <https://doi.org/10.1080/07388551.2020.1853672>
- Gonçalves, F., Silva, C., Ribeiro, A., & Cavaco-Paulo, A. (2018). 1-Aminoanthracene Transduction into Liposomes Driven by Odorant-Binding Protein Proximity. *ACS Applied Materials and Interfaces*, *10*(32), 27531–27539. <https://doi.org/10.1021/acsami.8b10158>
- Guex, N., & Peitsch, M. C. (1997). SWISS-MODEL and the Swiss-PdbViewer: An environment for comparative protein modeling. *Electrophoresis*, *18*(15), 2714–2723. <https://doi.org/10.1002/elps.1150181505>
- Guiraudie-Capraz, G., Clot-Faybesse, O., Pageat, P., Malosse, C., Cain, A. H., Ronin, C., & Nagnan-Le Meillour, P. (2005). Heterologous expression of piglet odorant-binding protein in *Pichia pastoris*: a comparative structural and functional characterization with native forms. *Journal of Biotechnology*, *117*(1), 11–19. <https://doi.org/10.1016/j.jbiotec.2005.01.005>
- Habib, M. K. (2007). Controlled biological and biomimetic systems for landmine detection. *Biosensors and Bioelectronics*, *23*(1), 1–18. <https://doi.org/10.1016/j.bios.2007.05.005>
- Huang, F., Wei, Q., & Cai, Y. (2012). Surface functionalization of polymer nanofibers. In *Functional Nanofibers and their Applications* (pp. 92–118). Elsevier. <https://doi.org/10.1533/9780857095640.1.92>

- Ioannou, J. C., Donald, A. M., & Tromp, R. H. (2015). Characterising the secondary structure changes occurring in high density systems of BLG dissolved in aqueous pH 3 buffer. *Food Hydrocolloids*, *46*, 216–225. <https://doi.org/10.1016/j.foodhyd.2014.12.027>
- Kong, J., & Yu, S. (2007). Fourier transform infrared spectroscopic analysis of protein secondary structures. *Acta Biochimica et Biophysica Sinica*, *39*(8), 549–559. <https://doi.org/10.1111/j.1745-7270.2007.00320.x>
- Lacazette, E., Gachon, A. M., & Pitiot, G. (2000). A novel human odorant-binding protein gene family resulting from genomic duplicons at 9q34: Differential expression in the oral and genital spheres. *Human Molecular Genetics*, *9*(2), 289–301. <https://doi.org/10.1093/hmg/9.2.289>
- Leal, W. S. (2013). Odorant reception in insects: Roles of receptors, binding proteins, and degrading enzymes. *Annual Review of Entomology*, *58*(September 2012), 373–391. <https://doi.org/10.1146/annurev-ento-120811-153635>
- Liu, X. Q., Jiang, H. B., Liu, Y., Fan, J. Y., Ma, Y. J., Yuan, C. Y., Lou, B. H., & Wang, J. J. (2020). Odorant binding protein 2 reduces imidacloprid susceptibility of *Diaphorina citri*. *Pesticide Biochemistry and Physiology*, *168*(March), 104642. <https://doi.org/10.1016/j.pestbp.2020.104642>
- Loutfi, A., Coradeschi, S., Mani, G. K., Shankar, P., & Rayappan, J. B. B. (2015). Electronic noses for food quality: A review. *Journal of Food Engineering*, *144*, 103–111. <https://doi.org/10.1016/j.jfoodeng.2014.07.019>
- Lu, Y., Zhang, D., Zhang, Q., Huang, Y., Luo, S., Yao, Y., Li, S., & Liu, Q. (2016). Impedance spectroscopy analysis of human odorant binding proteins immobilized on nanopore arrays for biochemical detection. *Biosensors and Bioelectronics*, *79*, 251–257. <https://doi.org/10.1016/j.bios.2015.12.047>
- Malpeli, G., Folli, C., Cavazzini, D., Sartori, G., & Berni, R. (n.d.). *Purification and Fluorescent Titration of Cellular Retinol-Binding Protein*.

- Paolini, S., Tanfani, F., Fini, C., Bertoli, E., & Pelosi, P. (n.d.-a). *Porcine odorant-binding protein: structural stability and ligand affinities measured by Fourier-transform infrared spectroscopy and fluorescence spectroscopy*.
- Paolini, S., Tanfani, F., Fini, C., Bertoli, E., & Pelosi, P. (n.d.-b). *Porcine odorant-binding protein: structural stability and ligand affinities measured by Fourier-transform infrared spectroscopy and fluorescence spectroscopy*.
- Pelosi, P. (2001). The role of perireceptor events in vertebrate olfaction. *Cellular and Molecular Life Sciences*, 58(4), 503–509. <https://doi.org/10.1007/PL00000875>
- Pelosi, P., Baldaccini, N. E., & Pisanelli, A. M. (1982). Identification of a specific olfactory receptor for 2-isobutyl-3-methoxypyrazine. In *Biochem. J* (Vol. 201).
- Pelosi, P., Mastrogiacomo, R., Iovinella, I., Tuccori, E., & Persaud, K. C. (2014). Structure and biotechnological applications of odorant-binding proteins. In *Applied Microbiology and Biotechnology* (Vol. 98, Issue 1, pp. 61–70). Springer Verlag. <https://doi.org/10.1007/s00253-013-5383-y>
- Pelosi, P., Zhu, J., & Knoll, W. (2018). From radioactive ligands to biosensors: binding methods with olfactory proteins. In *Applied Microbiology and Biotechnology* (Vol. 102, Issue 19, pp. 8213–8227). Springer Verlag. <https://doi.org/10.1007/s00253-018-9253-5>
- Sankaran, S., Panigrahi, S., & Mallik, S. (2011). Odorant binding protein based biomimetic sensors for detection of alcohols associated with Salmonella contamination in packaged beef. *Biosensors and Bioelectronics*, 26(7), 3103–3109. <https://doi.org/10.1016/j.bios.2010.07.122>
- Sawyer, L., & Kontopidis, G. (n.d.). *The core lipocalin, bovine L-lactoglobulin*. www.elsevier.com/locate/bba
- Scorsone, E., Manai, R., Cali, K., Ricatti, M. J., Farno, S., Persaud, K., & Mucignat, C. (2021). Biosensor array based on ligand binding proteins for narcotics and explosives detection. *Sensors and Actuators, B: Chemical*, 334(January), 129587. <https://doi.org/10.1016/j.snb.2021.129587>

- Seidman, C. E., Struhl, K., Sheen, J., & Jessen, T. (2001). Introduction of plasmid DNA into cells. *Current Protocols in Molecular Biology / Edited by Frederick M. Ausubel ... [et Al.], Chapter 1*, 1–10. <https://doi.org/10.1002/0471142727.mb0108s37>
- Silva, C., Matamá, T., Azoia, N. G., Mansilha, C., Casal, M., & Cavaco-Paulo, A. (2014a). Odorant binding proteins: A biotechnological tool for odour control. *Applied Microbiology and Biotechnology*, *98*(8), 3629–3638. <https://doi.org/10.1007/s00253-013-5243-9>
- Silva, C., Matamá, T., Azoia, N. G., Mansilha, C., Casal, M., & Cavaco-Paulo, A. (2014b). Odorant binding proteins: A biotechnological tool for odour control. *Applied Microbiology and Biotechnology*, *98*(8), 3629–3638. <https://doi.org/10.1007/s00253-013-5243-9>
- Sorokowska, A., Sorokowski, P., & Havlíček, J. (2016). Body odor based personality judgments: The effect of fragranced cosmetics. *Frontiers in Psychology*, *7*(APR), 1–8. <https://doi.org/10.3389/fpsyg.2016.00530>
- Staiano, M., D'Auria, S., Varriale, A., Rossi, M., Marabotti, A., Fini, C., Stepanenko, O. v., Kuznetsova, I. M., & Turoverov, K. K. (2007). Stability and dynamics of the porcine odorant-binding protein. *Biochemistry*, *46*(39), 11120–11127. <https://doi.org/10.1021/bi7008129>
- Tegoni, M., Pelosi, P., Vincent, F., Spinelli, S., Campanacci, V., Grolli, S., Ramoni, R., & Cambillau, C. (n.d.). *Mammalian odorant binding proteins*. www.elsevier.com/locate/bba
- Vogt, R. G., & Carolina, S. (2005). 3. 15 Molecular Basis of Pheromone Detection in Insects. *Biochemistry*.
- Wang, Q., Liu, J. T., Zhang, Y. J., Chen, J. L., Li, X. C., Liang, P., Gao, X. W., Zhou, J. J., & Gu, S. H. (2021). Coordinative mediation of the response to alarm pheromones by three odorant binding proteins in the green peach aphid *Myzus persicae*. *Insect Biochemistry and Molecular Biology*, *130*(October 2020), 103528. <https://doi.org/10.1016/j.ibmb.2021.103528>
- Xiong, W., Gao, S., Lu, Y., Wei, L., Mao, J., Xie, J., Cao, Q., Liu, J., Bi, J., Song, X., & Li, B. (2019). Latrophilin participates in insecticide susceptibility through positively regulating CSP10 and partially compensated by OBPC01 in *Tribolium castaneum*. *Pesticide Biochemistry and*

Physiology, 159(December 2018), 107–117.
<https://doi.org/10.1016/j.pestbp.2019.06.005>

Zalewska, A., Pawłowski, W., & Tomaszewski, W. (2013). Limits of detection of explosives as determined with IMS and field asymmetric IMS vapour detectors. *Forensic Science International*, 226(1–3), 168–172. <https://doi.org/10.1016/j.forsciint.2013.01.005>

Zhang, X., Cheng, J., Wu, L., Mei, Y., Jaffrezic-Renault, N., & Guo, Z. (2018). An overview of an artificial nose system. *Talanta*, 184(January), 93–102.
<https://doi.org/10.1016/j.talanta.2018.02.113>

7. Supplementary Information

7.1. Calibration curve of β -Citronellol:

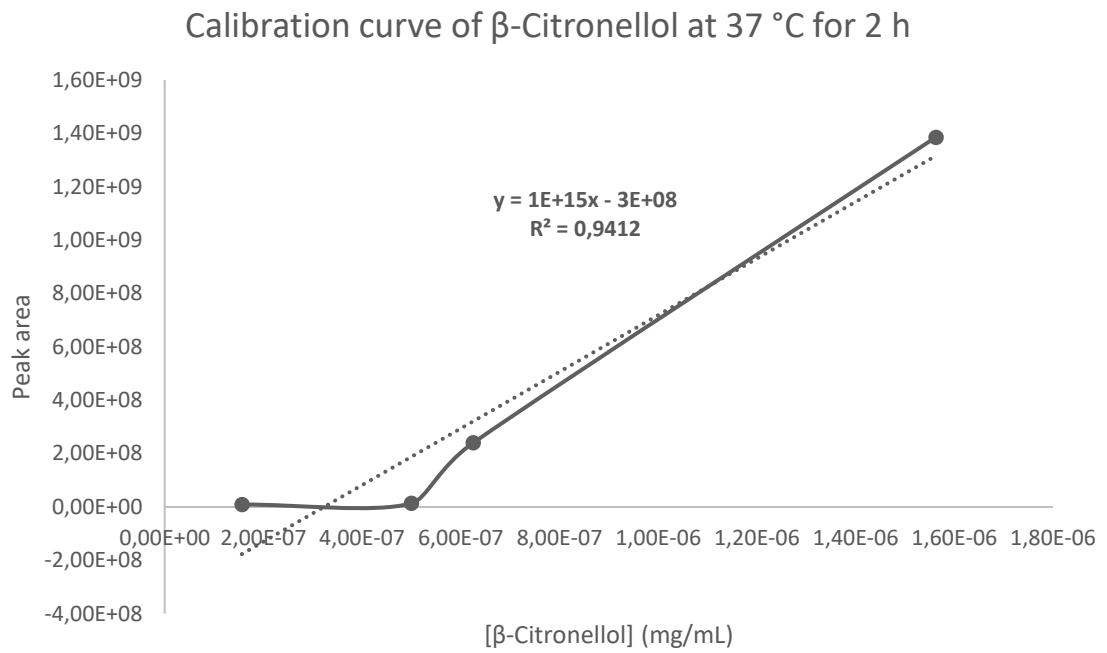


Figure SI 1- Calibration curve of β -Citronellol at 37 °C for 2 h of SPME exposition time.

7.2. GC data

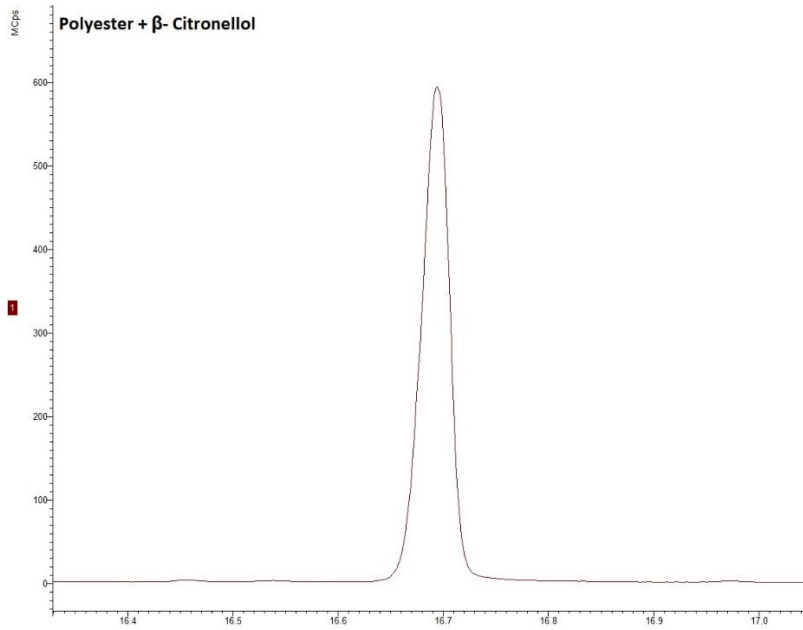


Figure SI 2- GC spectra of polyester fabric incubated with β - citronellol at 37 °C for 2 h of SPME exposition time at 37 °C for 2 h of SPME exposition time

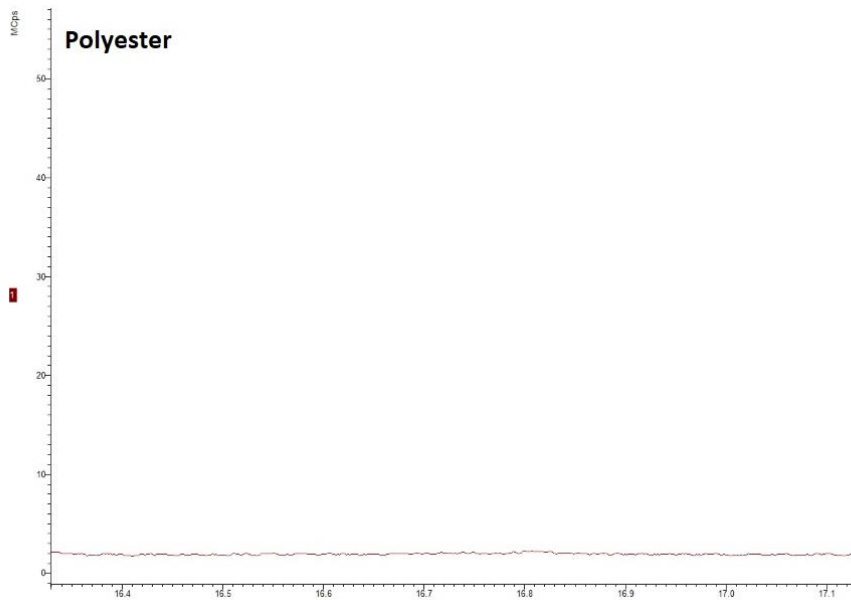
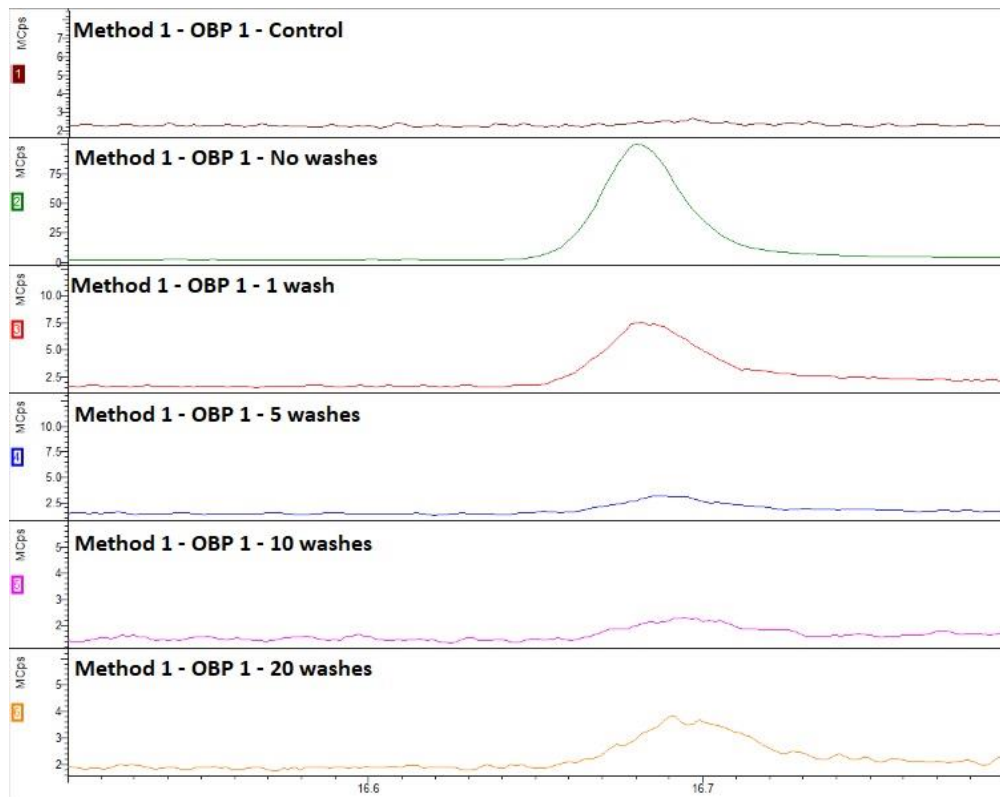
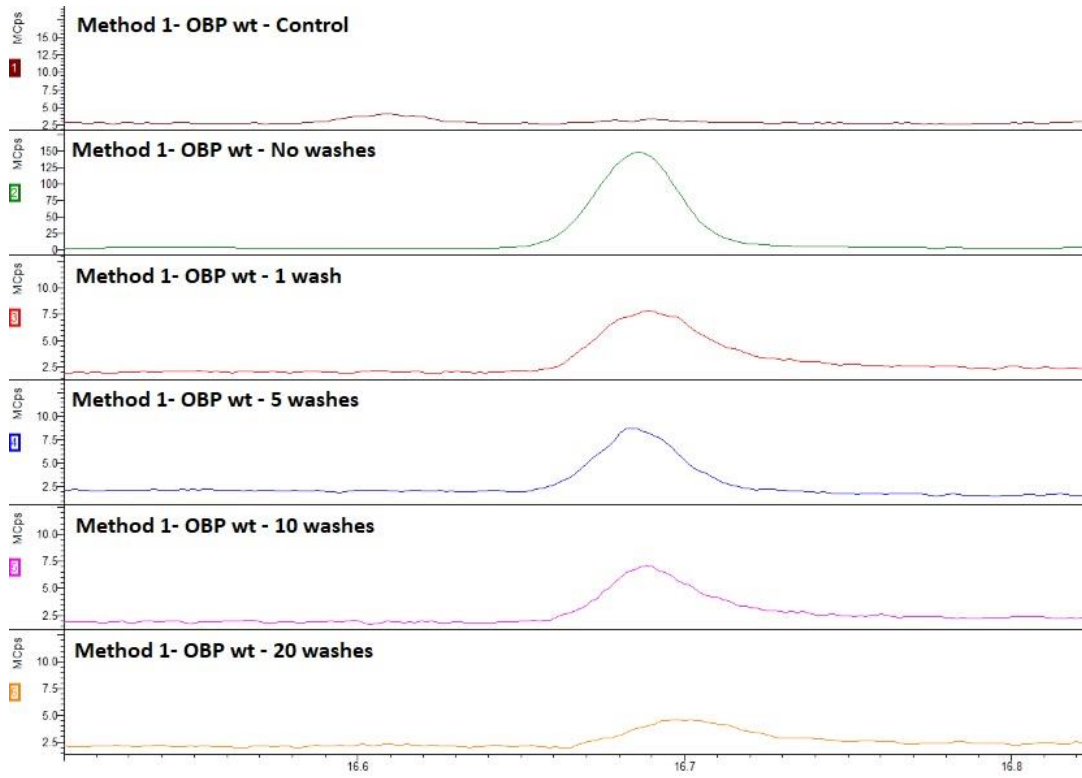


Figure SI 3- GC spectra of polyester fabric incubated at 37 °C for 2 h of SPME exposition time at 37 °C for 2 h of SPME exposition time.



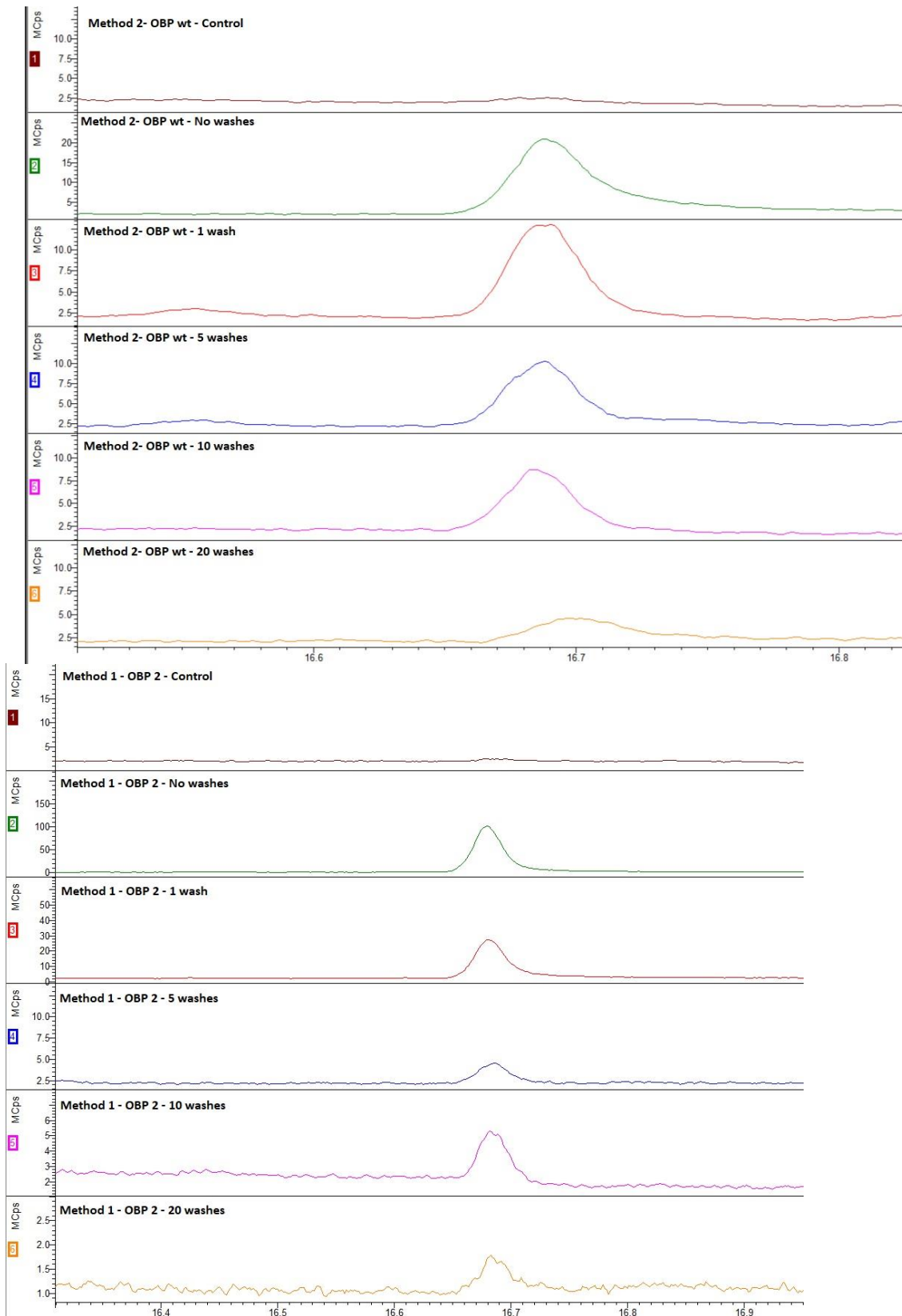


Figure SI 4- GC spectra from functionalization of polyester fabrics with OBP/ β -citronellol complex by method 1; impregnation incubated at 37 °C for 2 h of SPME exposition time.

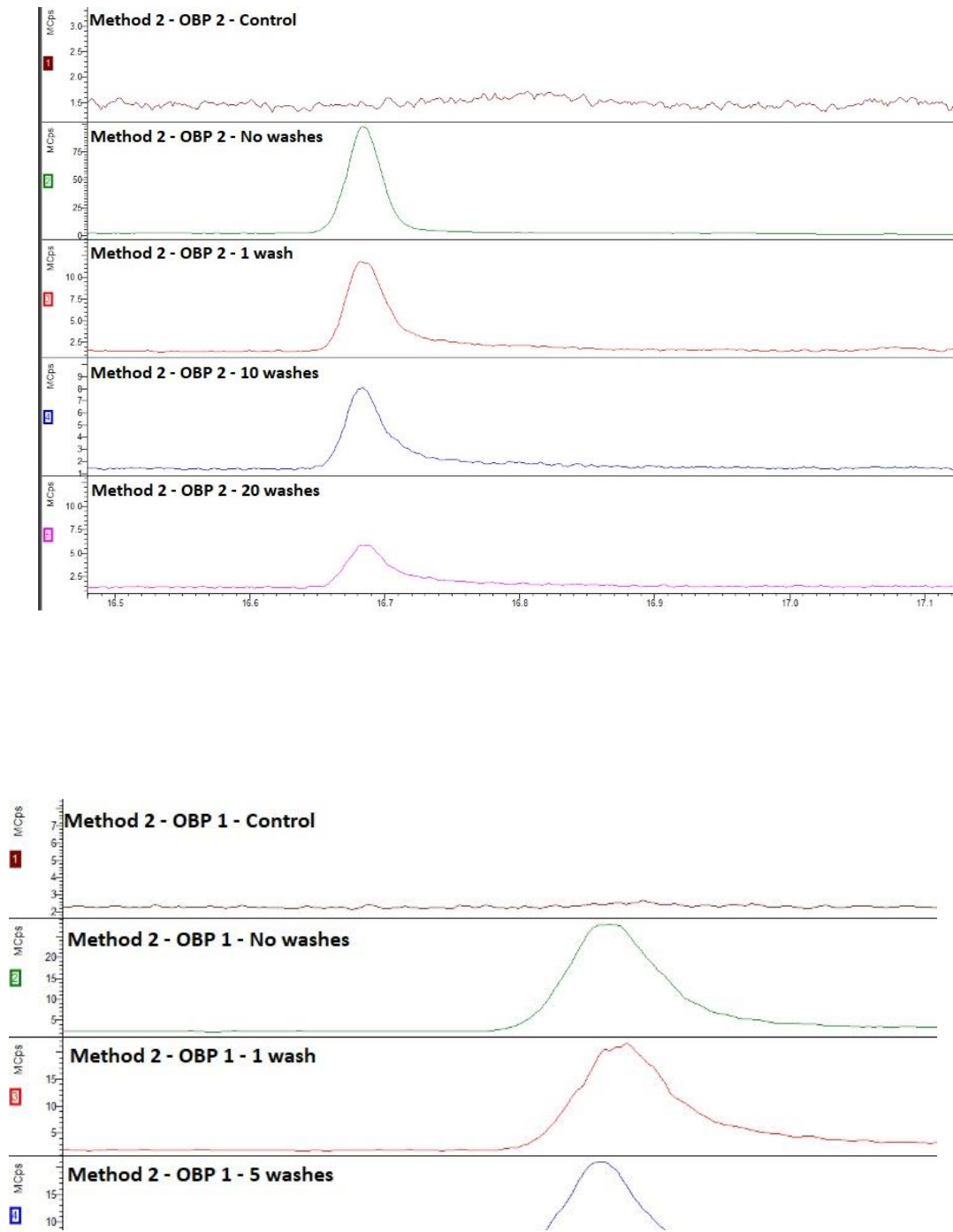


Figure SI 5- GC spectra from functionalization of polyester fabrics with OBP/ β -citronellol complex by method 2: Spray incubated at 37 °C for 2 h of SPME exposition time.